Precambrian Research 294 (2017) 189–213

Contents lists available at ScienceDirect

Precambrian Research

journal homepage: www.elsevier.com/locate/precamres

A mantle plume origin for the Palaeoproterozoic Circum-Superior Large Igneous Province

T. Jake R. Ciborowski [a,b,*], Matthew J. Minifie [b], Andrew C. Kerr [b], Richard E. Ernst [c,d], Bob Baragar [e], Ian L. Millar [f]

[a] School of Environment and Technology, University of Brighton, Brighton BN2 4GJ, UK
[b] School of Earth and Ocean Sciences, Cardiff University, Main Building, Park Place, Cardiff CF10 3AT, UK
[c] Department of Earth Sciences, Carleton University, Ottawa, Ontario K1S 5B6, Canada
[d] Faculty of Geology and Geography, Tomsk State University, pr. Lenina 36, Tomsk 634050, Russia
[e] Geological Survey of Canada, 601 Booth Street, Ottawa, Ontario K1A 0E8, Canada
[f] NERC Isotope Geosciences Laboratory, Kingsley Dunham Centre, Keyworth, Nottingham NG12 5GG, UK

ARTICLE INFO

Article history:
Received 14 October 2016
Revised 24 January 2017
Accepted 5 March 2017
Available online 09 March 2017

ABSTRACT

The Circum-Superior Large Igneous Province (LIP) consists predominantly of ultramafic-mafic lavas and sills with minor felsic components, distributed as various segments along the margins of the Superior Province craton. Ultramafic-mafic dykes and carbonatite complexes of the LIP also intrude the more central parts of the craton. Most of this magmatism occurred ~1880 Ma. Previously a wide range of models have been proposed for the different segments of the CSLIP with the upper mantle as the source of magmatism.

New major and trace element and Nd-Hf isotopic data reveal that the segments of the CSLIP can be treated as a single entity formed in a single tectonomagmatic environment. In contrast to most previous studies that have proposed a variety of geodynamic settings, the CSLIP is interpreted to have formed from a single mantle plume. Such an origin is consistent with the high MgO and Ni contents of the magmatic rocks, trace element signatures that similar to oceanic-plateaus and ocean island basalts and εNd-εHf isotopic signatures which are each more negative than those of the estimated depleted upper mantle at ~1880 Ma. Further support for a mantle plume origin comes from calculated high degrees of partial melting, mantle potential temperatures significantly greater than estimated ambient Proterozoic mantle and the presence of a radiating dyke swarm. The location of most of the magmatic rocks along the Superior Province margins probably represents the deflection of plume material by the thick cratonic keel towards regions of thinner lithosphere at the craton margins. The primary magmas, generated by melting of the heterogeneous plume head, fractionated in magma chambers within the crust, and assimilated varying amounts of crustal material in the process.

© 2017 The Authors. Published by Elsevier B.V. This is an open access article under the CC BY license (http://creativecommons.org/licenses/by/4.0/).

1. Introduction

Large Igneous Provinces (LIPs) represent large volume (>0.1 Mkm^3; frequently above >1 Mkm^3), mainly mafic (-ultramafic) magmatic events of intraplate affinity, that occur in both continental and oceanic settings, and are typically of short duration (<5 myr) or consist of multiple short pulses over a maximum of a few 10 s of m.y. (Coffin and Eldholm, 1994, 2005; Bryan and Ernst, 2008; Bryan and Ferrari, 2013; Ernst, 2014 and references therein). They comprise volcanic packages (flood basalts), and a plumbing system of dyke swarms, sill complexes, layered intrusions, and crustal underplate. LIPs can also be associated with silicic magmatism (including dominantly silicic events termed Silicic LIPs, or SLIPs), carbonatites and kimberlites. LIPs occur at a rate of approximately every ~20 myr back at least to 2.5 Ga (Ernst et al., 2005), and are known in the Archean, more sparsely due to poorer preservation (e.g. Ernst, 2014). LIPs have been used to constrain pre-Phanerozoic palaeocontinental reconstructions (e.g., Bleeker and Ernst, 2006; Soderlund et al., 2010), illuminate large-scale mantle processes (e.g., Coffin and Eldholm, 2005; Bryan and Ferrari, 2013), and understand the evolution of the biosphere (e.g., Sobolev et al., 2011; Ciborowski and Kerr, 2016).

Currently, the majority of LIPs in the geological record are thought to be the result of mantle plume-driven magmatism (see reviews in Kerr, 2014; Ernst, 2014). However, other processes for LIP formation have been proposed (Ernst, 2014), including mantle

* Corresponding author at: School of Environment and Technology, University of Brighton, Brighton BN2 4GJ, UK.
E-mail address: j.ciborowski@brighton.ac.uk (T. Jake R. Ciborowski).

http://dx.doi.org/10.1016/j.precamres.2017.03.001
0301-9268/© 2017 The Authors. Published by Elsevier B.V.
This is an open access article under the CC BY license (http://creativecommons.org/licenses/by/4.0/).

insulation (e.g., Anderson, 1982; Coltice et al.; 2009), edge-driven convection (King and Anderson, 1995; King, 2007), bolide impact (Ingle and Coffin, 2004; Jones, 2005), and mantle delamination (Anderson, 2000; Elkins-Tanton, 2007).

A belt of 1864–1884 Ma mafic–ultramafic rocks surrounds much of the Superior craton, the "Circum Superior belt" of Baragar and Scoates (1987) and subsequently studied by a number of researchers (e.g., Ernst and Buchan, 2001; Heaman et al., 2009). Remarkably extensive, and with relatively tight age concentrations, this belt is now recognized to constitute the Circum-Superior LIP. The belt continues for more than 3400 km and includes magmatism in (1) the Labrador Trough ("Cycle 2") on the east; (2) the Cape Smith belt (Chukotat volcanics) and eastern Hudson Bay (Sleeper Island and Haig sills); (3) the Thompson and Fox River belts (including the Molson dykes and Fox River sill) on the northwest, and (4) the Marquette Range Supergroup in the southern margin of the Superior craton (Fig. 6n; event #8 in Ernst and Buchan, 2004 and references therein; Mungall, 2007; Heaman et al., 2009; Ernst and Bell, 2010). The portion in the northwestern Superior craton (Thompson Promontory) has been termed the "Molson Igneous Events" by Heaman et al. (2009) and would include coeval Pickle Crow dykes that cut across the interior of the western Superior craton (Buchan et al., 2003). The observation that most of this LIP was emplaced along the Superior cratonic margin during the development of adjacent orogens (trans-Hudson, New Quebec, and Penokean) associated with pending ocean closure led to plate boundary models involving back-arc rifting or pull-apart basins produced by oblique convergence (e.g., see discussion in Heaman et al., 2009). However, the presence of a radiating swarm consisting of Molson dykes, Pickle Crow and Fort Albany dykes defines a potential plume centre in the Thompson Promontory region (Hamilton and Stott, 2008; Hamilton et al., 2009; Ernst and Buchan 2001).

Only a few segments of the CSLIP have previously been studied geochemically. Thus, the tectonomagmatic environment of formation of the igneous rocks of the CSLIP is far from clear, with previous models suggesting a range of settings such as mid-ocean ridge spreading, back-arc basin rifting, foredeep basin flexing, arc volcanism and mantle plume volcanic activity (e.g., Desharnais, 2005; Heaman et al., 2009). This study represents the first characterisation of the geochemistry and isotopic composition of all the segments of the CSLIP and will assess whether their mode of formation and petrogenesis is consistent with derivation from a mantle plume.

2. Overview of the Circum-Superior Large Igneous Province

2.1. The Superior Province

The predominantly Archaean (mostly ~3.1 to 2.7 Ga) Superior Province is divided into a number of volcano- plutonic, metasedimentary, plutonic, and high grade gneiss subprovinces (e.g. Card and Ciesielski, 1986). The central Superior Province is largely composed of alternating volcano-plutonic and metasedimentary subprovinces which are surrounded by high grade gneiss subprovinces. The volume of Proterozoic volcanic rocks, mafic dyke swarms and alkalic rock-carbonatite complexes is minimal compared to that of Archaean rocks.

Orogenic belts of Proterozoic age circumscribe most of the Superior Province and mark the collision zones between the Superior Province and other Archaean provinces or Proterozoic terranes (e.g., Schulz and Cannon, 2007). The margins of the Superior Province also comprise Palaeoproterozoic volcanic and sedimentary sequences of broadly similar stratigraphy and lithologies (e.g. Dimroth et al., 1970; Gibb and Walcott, 1971; Baragar and Scoates, 1981). Similar successions distributed around the Superior Province margin have been grouped together by Baragar and Scoates (1987) and have become known as the 'Circum-Superior Belt'.

2.2. The Circum-Superior Belt

The nine remnant segments of the Circum-Superior Belt (Fig. 1) are unevenly distributed around the Superior Province margin. These segments are the Cape Smith Belt, Eastern Hudson Bay Islands, Hudson Bay Lowlands, Fox River Belt, Thompson Nickel Belt (and Molson dykes), Lake Superior area, Mistassini-Otish Group, Southern Labrador Trough, and Labrador Trough (Baragar and Scoates, 1981). The potentially continuous nature of the Circum-Superior Belt is obscured by the Hudson Bay, Phanerozoic sediments and Grenvillian deformation.

Not all the segments which constitute the Circum-Superior Belt contain related magmatic rocks (e.g., Southern Labrador Trough, and the Mistassini-Otish Group). However, in those segments that contain magmatic rocks, recent advances in U-Pb zircon/baddeleyite geochronology have shown that there is a marked synchronicity between the magmatic rocks, with ages ranging from 1885 to 1864 Ma (Ernst and Buchan, 2004; Ernst and Bleeker, 2010 and references therein). This synchronicity (Table 1; Fig. 2), combined with the widespread extent of magmatism along the cratonic margins and its predominant mafic-ultramafic composition, led Ernst and Buchan (2004) to classify the 1885–1864 Ma Circum-Superior Belt magmatic rocks as a large igneous province (LIP) (Coffin and Eldholm, 1994; Bryan and Ernst, 2008; Ernst, 2014) termed the Circum-Superior LIP. More recent U-Pb dating (Ernst and Bell, 2010) has led to the recognition of ~1880 Ma magmatism in the interior of the craton which is broadly coeval to that preserved in the Circum-Superior Belt (Table 1).

2.3. The Circum-Superior LIP

2.3.1. Cape Smith Belt

The Cape Smith Belt extends ~375 km across nearly the entire Ungava Peninsula of northern Quebec (Fig. 1) and consists of volcano-sedimentary and plutonic suites structurally emplaced onto the Archaean basement of the Superior Province. The belt can be divided into two domains separated by the Bergeron Fault (Picard et al., 1990). The parautochthonous southern domain is composed of the Povungnituk and Chukotat Groups while the Spartan, Parent and Watts Groups make up the allochthonous northern domain (St-Onge et al., 2000).

2.3.1.1. Chukotat group. The Chukotat Group of the Cape Smith Belt is composed mainly of ultramafic to mafic volcanic and intrusive rocks with minor intercalated fine-grained siliciclastic sediment. The thickness of the Chukotat Group varies between ~4 and 5 km in the central and eastern portions of the Cape Smith Belt (Mungall, 2007) to between ~7 and 15 km on Smith Island and the Ottawa Islands (Baragar, 2008). U-Pb dating of gabbroic sills, which are interpreted to have fed the Chukotat volcanism, has yielded ages of 1887 + 39/−11 Ma and 1882.7 ± 1.3 Ma (Wodicka et al., 2002; Randall, 2005).

The volcanic rocks of the Chukotat Group are predominantly basaltic pillow lavas and subaqueous flows although massive flows with ropy surfaces and polyhedral jointing are not uncommon (Lesher, 2007). Layered flows are also present in the Chukotat Group, particularly on Smith Island and the Ottawa Islands (Baragar, 2008). Three distinct petrographic types of basalts are found in the Chukotat Group i) olivine-phyric basalts with MgO ~12–19 wt%; ii) clinopyroxene-phyric basalts with MgO ~8–

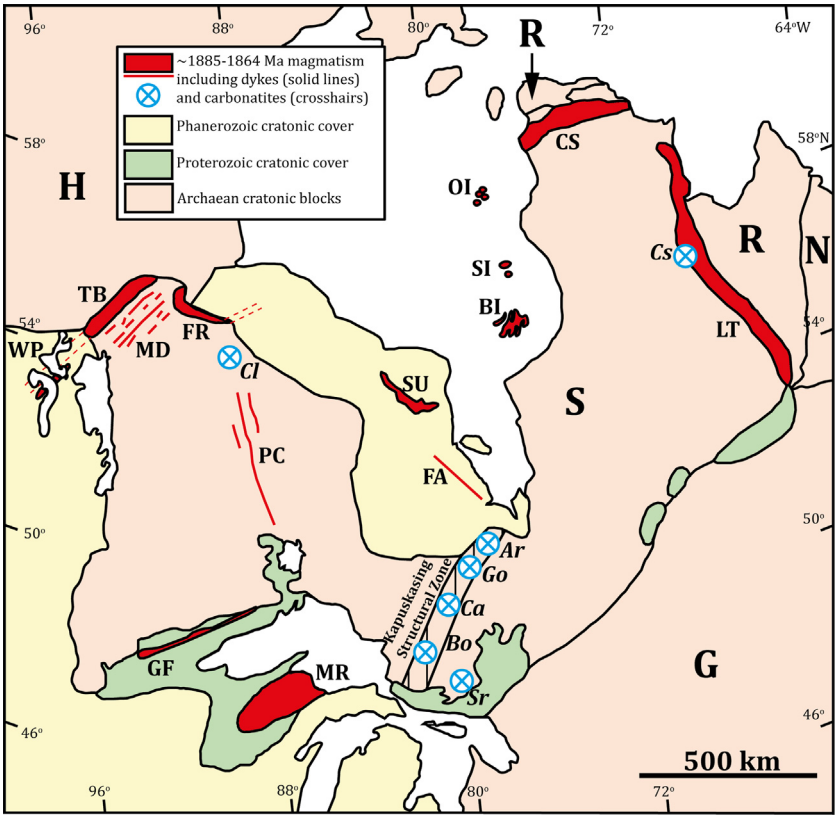

Fig. 1. Map of the Superior Province showing the location of the various segments of the Circum-Superior Belt and Circum-Superior LIP. Adapted from Baragar and Scoates (1981). Tectonic elements of Laurentia: G – Grenville Province, H – Hearne Craton, N – Nain Craton, R – Rae Craton, S – Superior Craton; ~1885–1864 Ma mafic magmatism: BI – Belcher Islands, CS – Cape Smith Belt, FA – Fort Albany dykes, FR – Fox River Belt, GF – Gunflint Formation, LT – Labrador Trough, MR – Marquette Range Supergroup, MD – Molson dykes, OI – Ottawa Islands, PC – Pickle Crow dyke, SI – Sleeper Islands, SU – Sutton Inlier, TB – Thompson Nickel Belt, WP – Winnipegosis Belt; ~1885–1864 Ma carbonatites: Ar – Argor, Bo – Borden, Ca – Cargill, Cl – Carp Lake, Cs – Castignon Lake, Go – Goldray, Sr – Spanish River.

12 wt%; and iii) plagioclase-phyric basalts with MgO ~4–7 wt% (Baragar, 2008).

2.3.1.2. Raglan formation. Numerous ultramafic-mafic bodies intrude into the lower Chukotat Group and underlying Povungnituk Group, which define a regionally mappable unit over ~85 km in length which Lesher et al. (1999) named the Raglan Formation. Lesher (2007) has divided the Raglan bodies into two different groups: i) thick but laterally restricted units composed mainly of massive olivine mesocumulate (peridotite) and ii) laterally restricted units of olivine orthocumulate (olivine-pyroxenite) and gabbros. The age of the Raglan Formation ranges between 1887 + 39/-11 Ma and 1870 ± 4 Ma (St-Onge et al., 2000; Wodicka et al., 2002).

2.3.1.3. The Expo-Ungava Intrusive Suite. The Expo-Ungava Intrusive Suite is a suite of ultramafic-mafic intrusive bodies in the Cape Smith Belt (Randall, 2005; Mungall, 2007). The Suite occurs at a lower stratigraphic level within the Povungnituk Group than the Raglan Formation and covers a strike length of ~32 km. Stacked sills, large dykes, steeply inclined pipes, ovoid conduits and trough-shaped discordant bodies are present in the Suite and are predominantly olivine melagabbronorites with pyroxenite, peridotite and dunite lithologies also present. The age of the Expo Ungava Intrusive Suite has been determined by U-Pb zircon dating of a melagabbro which yielded an age of 1882.7 ± 1.3 Ma (Randall, 2005).

2.3.2. Hudson Bay region

2.3.2.1. The Belcher Islands. The Belcher Islands lie ~150 km west of the Ungava Peninsula (Fig. 1) and are dominated by numerous sedimentary units and two volcanic formations. The lowermost 'Kasegalik' formation consists of a maximum of 1200 m thick evaporitic and stromatolitic dolostones (Ricketts and Donaldson, 1981). Overlying the Kasegalik Formation is the Eskimo Formation, a unit of columnar- jointed flood basalts which attain a maximum thickness of 900 m. Overlying the Eskimo Formation are a thick sequence of sediments that are in turn overlain by pillowed and massive basalt lava flows and volcanoclastic deposits of the <1600 m thick Flaherty Formation (Ricketts et al., 1982).

Doleritic-gabbroic sills, known as the Haig sills, which have maximum thicknesses of ~300 m, intrude the Eskimo Formation and overlying sediments up to the base of the Flaherty Formation (Baragar, 2007a). These sills are considered to have fed the Flaherty Formation lavas and are not thought to be related to the Eskimo Formation (Dimroth et al., 1970; Baragar, 2007a). Instead, the Eskimo Formation volcanics are thought to be c. 1998 Ma based on paleomagnetic correlation with the Minto dykes (Buchan et al., 1998).

No reliable age determinations have been obtained for the Flaherty Formation on the Belcher Islands. The only age comes from Todt et al. (1984) who obtained a Pb-Pb isochron age with a large error of 1960 ± 80 Ma. However, field relationships suggest that the Haig sills are the intrusive equivalent of the extrusive Flaherty Formation (Baragar, 2007b).

2.3.2.2. The Sleeper Islands. The Sleeper Islands consist of two major, and many smaller, islands which lie ~100 km north of the Belcher Islands. Unlike the Belcher Islands, the Sleeper Islands are dominated by a volcanic formation (Flaherty Formation) and associated sills (Baragar and Lamontagne, 1980). The Flaherty Formation basalts comprise both pillowed and massive flows and vary

Table 1
Age determinations for rocks belonging to the Circum-Superior LIP.

Suite	Method	Age (Ma)	Reference
Cape Smith Belt			
Raglan Formation gabbro	U-Pb zircon	1887^{+39}_{-11}	Wodicka et al. (2002)
Expo-Ungava Intrusive Suite gabbro	U-Pb zircon	1882.7 ± 1.3	Randall (2005)
Chukotat Group gabbro	U-Pb zircon	1870 ± 4	St-Onge et al. (1992)
Hudson Bay			
Flaherty Formation basalts	Pb-Pb isochron	1960 ± 80	Todt et al. (1984)
Hudson Bay Lowlands			
Fort Albany dolerite dyke	U-Pb baddeleyite	1870.7 ± 1.1	Hamilton and Stott (2008)
Fox River Belt			
Fox River Sill Marginal Zone gabbro	U-Pb zircon	$1882.9^{+1.5}_{-1.4}$	Heaman et al. (1986)
Thompson Nickel Belt			
South Setting Lake pyroxenite	U-Pb zircon	1880 ± 5	Hulbert et al. (2005)
Sulphide ores	Re-Os isochron	1885 ± 49	Hulbert et al. (2005)
Paint Lake pyroxenite sill	U-Pb zircon	1876.7 ± 5.1	Heaman et al. (2009)
Winnipegosis Belt			
Coarse grained mafic unit	U-Pb zircon	1864^{+6}_{-4}	Hulbert et al. (1994)
Mafic unit	U-Pb zircon	1870.3 ± 7.1	Waterton et al. (2017)
Molson dykes			
Granophyric Cross Lake dyke	U-Pb zircon	1883.7 ± 1.6	Heaman et al. (1986)
Olivine pyroxenite Cuthbert Lake dyke	U-Pb zircon	1883 ± 2	Heaman et al. (1986)
Cauchon Lake gabbro dyke	U-Pb zircon	1877^{+7}_{-4}	Halls and Heaman (2000)
Bear Island gabbro dyke	U-Pb zircon	1885.2 ± 2.1	Heaman et al. (2009)
Molson Lake gabbronorite dyke	U-Pb zircon	1884.5 ± 3.8	Heaman et al. (2009)
Carrot River gabbro dyke	U-Pb	1891 ± 4	Burnham et al. (2004)
Pickle Crow dyke			
Gabbroic portion of dyke	Ar-Ar hornblende	1876 ± 8	Buchan et al. (2003)
Lake Superior region			
Hemlock Formation rhyolite	U-Pb zircon	1874 ± 9	Schneider et al. (2002)
Lamprophyre on Little Presque Isle	Ar-Ar phlogopite	1877.2 ± 5.3	Craddock et al. (2007)
Gunflint Formation volcanic ash	U-Pb zircon	1874 ± 9	Fralick et al. (2002)
Labrador Trough			
Glomeroporphyry Montagnais gabbro	U-Pb zircon	1884.0 ± 1.6	Findlay et al. (1995)
Glomeroporphyry Montagnais gabbro	U-Pb zircon	1874 ± 3	Machado et al. (1997)
Douay Lake rhyodacite	U-Pb zircon	1870 ± 4	Machado et al. (1997)
Nimish Formation syenite cobbles	U-Pb zircon	1877.8 ± 1.3	Findlay et al. (1995)
Castignon Lake carbonatite dyke	U-Pb zircon	1880 ± 2	Cheve and Machado (1988)
Carbonatite complexes			
Borden Township	Pb-Pb isochron	1872 ± 13	Bell et al. (1987)
	Pb-Pb zircon	1882.0 ± 3.9	Rukhlov and Bell (2010)
Carb Lake	Pb-Pb zircon	1865 ± 22	Rukhlov and Bell (2010)
Cargill Township	U-Pb zircon	1907 ± 4	Sage (1988a)
	U-Pb zircon	1896.8 ± 1.4	Rukhlov and Bell (2010)
Castignon Lake	U-Pb zircon	1880 ± 2	Cheve and Machado (1988)
Goldray	U-Pb zircon	1886 ± 0.9	Rukhlov and Bell (2010)
	U-Pb zircon	1884 ± 2	Sage (1988b)
Spanish River	Ub-Pb baddeleyite	1880.6 ± 2.4	Rukhlov and Bell (2010)

from aphyric to feldspar-phyric types. Representatives of the Haig sills are also present on the Sleeper Islands (Baragar, 2007a). There is at least one gabbroic sill which outcrops along the eastern coast of the two major islands and on the many small islands off the eastern coast of the major islands. This Haig sill yielded a U-Pb baddeleyite age of 1870 ± 4 Ma (Hamilton et al., 2009).

2.3.2.3. Sutton Inlier. The Sutton Inlier occurs in an area near Sutton Lake (Fig. 1) where Archaean and Proterozoic rocks are exposed through the Palaeozoic cover (Bostock, 1971). Carbonates, greywackes, siltstones, an iron formation and intrusive mafic sills form the Proterozoic succession which unconformably overlies Archaean basement gneisses (Baragar and Scoates, 1981). Based on the similarity of pole positions for the three igneous suites, Schwarz and Freda (1983) suggested that the Sutton Inlier sills are coeval with the Flaherty Formation volcanic rocks and Haig sills of the Belcher and Sleeper Islands. The Sutton Inlier sills have been dated (U-Pb baddeleyite) at 1870 ± 2 Ma (Hamilton et al., 2009).

2.3.2.4. Fort Albany dykes. Hamilton and Stott (2008) have obtained a U-Pb baddeleyite age of 1870.7 ± 1.1 Ma from a dolerite dyke underneath Palaeozoic cover near Puskwuche Point on the west coast of James Bay (Fig. 1). Aeromagnetic data show that this dyke trends in a northwesterly direction and is colinear with another northwest trending dyke ~150 km northwest of Puskwuche Point. Together these dykes have been referred to as the Fort Albany dykes (Hamilton and Stott, 2008). Based on their trend and apparent convergence with the Molson and Pickle Crow dykes, Hamilton and Stott (2008) suggest that the Fort Albany dykes may form part of a radiating dyke swarm (part of the Pickle Crow – Molson swarm discussed above) that define a mantle plume centre just to the north of the Thompson Salient.

2.3.3. Fox River Belt

The Fox River Belt is an east-striking, north-dipping monoclinal supracrustal sequence in northern Manitoba (Fig. 1). The ~15 km thick stratigraphy is divided into three sedimentary and two vol-

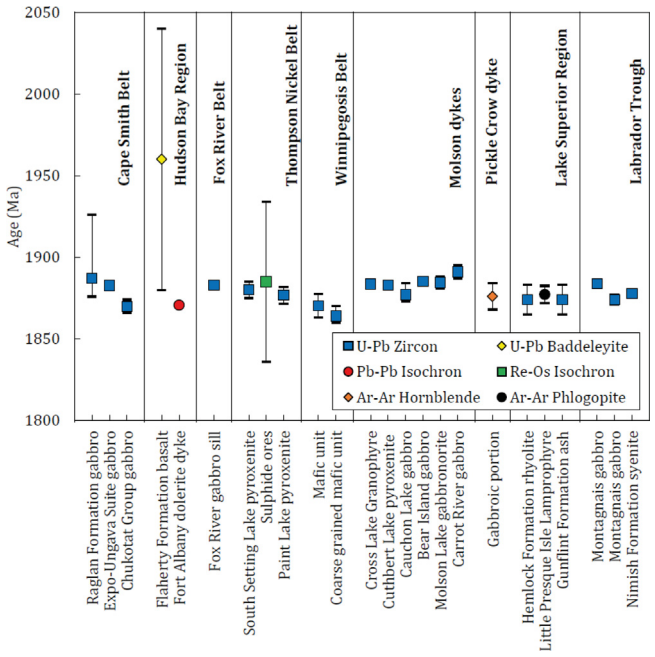

Fig. 2. Age determinations for rocks belonging to the Circum-Superior LIP. For data sources, see Table 1.

canic formations with two suites of intrusive rocks, unconformably overlying Archaean gneiss of the Superior Province (Scoates, 1981).

The ~2 km thick Lower Volcanic Formation comprises a range of pillowed and massive basalts, quartz basalts, clinopyroxenites, pyroxene-spinifex and plagioclase-phyric basalt flows (Scoates, 1981). The Upper Volcanic Formation (2.5–3.5 km thick) also consists of pillowed and massive basalt flows and layered differentiated flow units with olivine-clinopyroxenite (Scoates, 1981).

2.3.3.1. Fox River Belt intrusions. The ~2 km thick layered Fox River Sill intrudes the sedimentary units of the Fox River Belt and is thought to extend for >250 km in length, making it one of the largest ultramafic intrusions in the world (e.g. Hulbert et al., 2005). The layered sill comprises olivine-, clinopyroxene- and plagioclase-rich cumulate layers, with orthopyroxene in the upper cumulate layers and the common occurrence of plagioclase cumulate rocks capping the cyclic units. Hybrid Roof Zone rocks at the top of the intrusion are characterised by the presence of quartz-bearing granophyres (Scoates, 1981)

Other large (commonly differentiated) sills known as the Lower Intrusions which range from ~1.5 to 20 km in strike length and ~50 to 800 m in thickness are also found in the region. These intrusions usually consist of a peridotitic base overlain by a pyroxene-rich layer with an upper gabbronorite section (Desharnais, 2005). In addition to these sills a number of east-striking gabbroic dykes have also been recognized in the Fox River Belt region (Desharnais, 2005).

The most precise published age date obtained from the igneous rocks of the Fox River Belt comes from the Fox River Sill. Heaman et al. (1986) obtained a U-Pb zircon age of 1882.9 + 1.5/-1.4 Ma from a sample of vari-textured gabbro at the base of a cyclic unit. Heaman et al. (2009) reported a U-Pb zircon age of 1900 ± 14 Ma from one of the east-striking gabbroic dykes.

2.3.4. Lake Superior region

Palaeoproterozoic supracrustal rocks in the Lake Superior region form a discontinuous linear belt which extends from central Minnesota to eastern Ontario along the southern margin of the Superior Province. For this study only the Marquette Range Supergroup are of interest as it contains igneous rocks that are potentially part of the CSLIP.

2.3.4.1. Hemlock formation. The Marquette Range Supergroup (Fig. 1) is divided into four groups (Ojakangas et al., 2001). Of interest to this current study is the Menominee Group containing the volcanic rocks known as the Hemlock Formation which is dominated by massive and pillow basalts with subordinate agglomerates, rhyolites, tuffs and tuffaceous slates (Gair and Wier, 1956). The thickness of the Hemlock Formation is extremely variable and ranges from a minimum of 700 m to a maximum of 10 km (Wier, 1967). Another unit of volcanic rocks known as the Badwater Greenstone is also present in the Marquette and Menominee Ranges and are correlative with the Hemlock Formation (Sims, 1990). In the Gogebic Range the Emperor Volcanic Complex (Trent, 1976) lies at the same stratigraphic level as the Hemlock and Badwater volcanic rocks. The age of the Hemlock Formation has been determined by U-Pb zircon dating of a rhyolite flow to be 1874 ± 9 Ma (Schneider et al., 2002). Slightly older at 1891+/-3 Ma (U-Pb baddeleyite) is the Belleview metadiabase (Pietrzak-Renaud and Davis, 2014).

2.3.4.2. Kiernan sills. Two Kiernan sills intrude into the Hemlock Formation (Gair and Wier, 1956). The western sill is the larger of the two and is ~20 km long and ~0.7–5 km wide. The sill is differentiated, with a basal zone of serpentinised peridotite, a zone of metagabbro, an iron-rich transition zone and granophyric pockets. The eastern sill is ~10 km long and 1400 m wide and is composed of undifferentiated gabbro. There are currently no reliable age determinations for the Kiernan sills. However, field evidence and geochemical similarities suggest that the Kiernan sills are comagmatic and coeval with the extrusive Hemlock Formation (Ueng et al., 1988).

2.3.4.3. Little Presque Isle lamprophyres. On Little Presque Isle close to Marquette, two perpendicular, lamprophyric dykes have yielded an Ar-Ar plateau age of 1877 ± 5 Ma (Craddock et al., 2007). These dykes strike east-west and north-south in a small, ~3 km^2 outcrop.

2.3.4.4. Gunflint formation. The Gunflint Formation forms a ~175 km long, mostly sedimentary, belt north of Lake Superior (Fig. 1) with an average thickness of 120 m (Schmidt and Williams, 2003). The upper members of the formation contain volcanic ash beds (1878 ± 1.3 Ma (Fralick et al., 2002)) and basaltic lavas. The lavas are composed of massive and pillow basalts whose basaltic nature and limited extent suggests that they are an unlikely source of the ash deposits, though are likely to be of a similar age given their stratigraphic position.

2.3.5. Labrador Trough

2.3.5.1. Nimish Formation. The geology and lithostratigraphy of the ~800 km long Labrador Trough (Fig. 1) is dominated by two volcano-sedimentary sequences. Towards the west of the southern Labrador Trough, while the first cycle is significantly older than the CSLIP, the second cycle of volcanism is preserved within the 1878 ± 1.3 Ma Nimish Formation, an alkaline, mafic to felsic volcano-plutonic suite interbedded with the Sokoman Formation (Findlay et al., 1995).

2.3.5.2. Hellancourt formation. In the east part of the southern Labrador Trough, the Sokoman Formation is not as well represented as it is in the west, however, a ~5.5 km thick pile of basalt flows is preserved, known as the Willbob Formation. This formation comprises pillow basalt, columnar basalt, massive aphanitic basalt, massive dolerite, and basalt breccia and has been dated at

1885 ± 67 (Pb-Pb isochron) by Rohon et al. (1993). In the north of the Labrador Trough, the Hellancourt Formation is interpreted to be the northern equivalent to the Willbob basalts (Skulski et al., 1993). The Hellancourt Formation consists of a <100 m thick basal unit of plagioclase glomeroporphyritic, pillowed and massive basalt flows which is overlain by ~1000 m of aphyric massive and pillowed basalts and minor lapilli tuff.

2.3.5.3. Montagnais intrusions. Numerous sills of the Montagnais intrusions (1884–1874 Ma) are found at various stratigraphic levels of the second cycle in both the north and south of the Labrador Trough (Findlay et al., 1995). The sills mostly comprise gabbro, olivine gabbro, glomeroporphyritic gabbro and/or peridotite with ferrogabbro, quartz diorite and granodiorite (Skulski et al., 1993). Peridotitic sills are most common in a narrow belt in the eastern part of the central Labrador Trough (Baragar and Scoates, 1981).

2.3.6. Thompson Nickel Belt

The Thompson Nickel Belt (Fig. 1) forms a ~10–35 km wide northeast-trending belt along the northwest margin of the Superior Province that contains remnants of a Neoarchaean-Palaeoproterozoic continental margin (e.g., Layton-Matthews et al., 2007). The belt is comprised of a Proterozoic supracrustal sequence of metasediments and metavolcanics known as the Ospwagan Group (Scoates et al., 1977) which is intruded by numerous ultramafic bodies (e.g., Paktunc, 1984).

A large number of ~1878 Ma ultramafic bodies intrude the Ospwagan Group at various stratigraphic levels in a ~6 km wide zone along the western side of the Thompson Nickel Belt (Heaman et al., 2009). The bodies are lensoid to tabular in shape and range in width up to 1 km (Peredery, 1982) and can be traced for lengths of hundreds of metres (Layton-Matthews et al., 2007). Although highly serpentinised and metamorphosed to upper amphibolite facies (Burnham et al., 2004) the ultramafic intrusions commonly preserve a thin pyroxenitic basal zone with a thicker central zone of chromite-bearing olivine peridotites and dunites overlain by a thinner pyroxenitic upper zone (Peredery, 1982; Layton-Matthews et al., 2007).

A significant amount of felsic magmatism is known to be coeval with the ultramafic magmatism in the Thompson Nickel Belt. A number of examples of quartz diorite, granodiorite, granite and monzogranite plutons from the Setting Lake and Mystery Lake areas have yielded U-Pb ages ranging between 1891 and 1871 Ma (Zwanzig et al., 2003; Percival et al., 2004, 2005; Heaman et al., 2009).

2.3.7. Winnipegosis Belt

The Winnipegosis Belt (Fig. 1) is a >150 km long, northeast-trending greenstone belt consisting of sedimentary and volcanic rocks (Burnham et al., 2004; Waterton et al., 2017). The western margin of the Winnipegosis Belt is thought to be faulted against the sub-Palaeozoic southern extension of the Thompson Nickel Belt whilst the eastern margin is in unconformable contact with Superior Province gneisses (Burnham et al., 2004). In addition to various sedimentary rocks the belt comprises 1870.3 ± 7.1 Ma basalts and komatiites (Hulbert et al., 1994; Burnham et al., 2004; Waterton et al., 2017).

2.3.8. Molson dyke swarm

The Molson dykes (Fig. 1) form a large swarm extending over an area of ~26,000 km^2 (Heaman et al., 1986). They range in composition from dolerite-gabbro to pyroxenite and contain olivine, clinopyroxene, orthopyroxene, plagioclase and hornblende as initial crystallisation phases (Scoates and Macek, 1978). The dykes range in width from <1 to 60 m (Paktunc, 1987) and can be traced for hundreds of metres. The Molson dyke swarm is estimated to represent a magma volume of ~50,000 km^3 (Halls and Heaman, 2000). A total of seven dykes in the Molson swarm have been dated by U-Pb zircon. These ages range from 1900 to 1877 Ma with four of the seven dates lying between 1885 and 1883 Ma (e.g., Halls and Heaman, 2000; Burnham et al., 2004).

2.3.8.1. Pickle Crow dykes. The 1876 ± 8 Ma (U-Pb zircon) Pickle Crow dyke (Fig. 1) is an 80 m wide, northwest trending dolerite-gabbro dyke that can be traced for ~600 km across the interior of the Superior Province from near the Thompson Salient towards Lake Superior (Buchan et al., 2003). There are also two dykes parallel and adjacent to the Pickle Crow dyke which have been traced for 60 and 100 km. Based on geochronological data, and the apparently converging trends of the dykes, it has been proposed that the Pickle Crow dykes form part of a radiating dyke swarm with a convergence point to the north of the Thompson Salient and may have fed the ~1880 Ma magmatism in the Lake Superior region (Buchan et al., 2003; Minifie et al., 2013). The Fort Albany dykes continue the radiating pattern (Hamilton and Stott, 2008); in addition the E-W dykes associated with the Fox River sill (Heaman et al., 2009, as discussed above) could represent a further continuation of this radiating pattern.

2.3.9. Carbonatite complexes

A number of carbonatite complexes occur in the Superior Province, particularly in the Kapuskasing Structural Zone (Fig. 1) which have either been dated at ~1880 Ma or are considered likely to be of this age (Ernst and Bell, 2010). Apart from U-Pb (zircon) dating, little research has been carried out on these complexes that have a weighted mean U-Pb age of 1882 ± 1 Ma. A brief summary of these ages and available information on these carbonatite complexes is given in Electronic Appendix 1.

2.4. Summary

Various models for the formation of the CSLIP segments have been suggested and these include continental margin rifting, ocean floor spreading, back-arc basin rifting, arc volcanism, foredeep basin flexure, transtension in pull-apart basins along thinned continental margins, and mantle plume volcanism. More recent studies (e.g., Buchan et al., 2003; Desharnais, 2005; French et al., 2008; Heaman et al., 2009; Ernst and Bell, 2010) have interpreted the CSLIP as a single province and suggested possible modes of formation. Buchan et al. (2003), Desharnais (2005) and Minifie et al. (2013) advocated a mantle plume origin largely based on the presence of a possible radiating dyke swarm involving the Molson, Pickle Crow and Fort Albany dykes. French et al. (2008) and Heaman et al. (2009) dismissed a mantle plume origin and favoured passive upwelling of upper mantle asthenosphere along the thinned margins of the craton. Heaman et al. (2009) cited five main reasons against a mantle plume origin: i) the lack of a convincing radiating dyke swarm (since recognized); ii) lack of evidence for uplift prior to volcanism; iii) lack of a hotspot track (but such post-plume hot spot tracks are rarely observed in cratons); iv) widely dispersed segments of volcanism along a continental margin; and v) presence of mid-ocean ridge basalt (MORB)-like geochemical signatures and absence of ocean island basalt (OIB) geochemical signatures. In this study we use new geochemical data to reassess the petrogenesis and tectonomagmatic origin of the CSLIP (Electronic Appendix 2).

3. Geochemistry

This study represents the first attempt at collating representative geochemical data for all of the constituent suites of the CSLIP.

Table 2
Summary table showing the whole-rock geochemistry of the Circum-Superior LIP suites studied here.

	Badwater Greenstone Belt	Chukotat Group	Emperor Volcanic Complex	Flaherty Formation	Fox River Belt	Gunflint Formation	Haig sill	Hellancourt Formation	Hemlock Formation	Kiernan sills	Molson dykes	Pickle Crow dyke	Thompson Nickel Belt	Winnipegosis Belt
MgO (wt %)	3.85–8.64	6.42–18.99	2.44–8.15	4.91–7.89	4.42–37.5	4.21–6.24	5.20–7.35	6.00–9.65	0.49–8.32	6.65–10.47	5.99–20.45	6.47–7.71	22.75–36.86	6.68–25.34
Fe_2O_3 (wt%)	12.19–14.96	10.86–16.75	3.74–13.59	13.95–18.68	6.88–16.23	12.15–18.2	13.31–21.07	8.49–15.12	1.15–25.8	10.14–16.09	10.93–16.18	8.82–14.93	7.15–17.10	11.46–16.15
SiO_2 (wt %)	47.73–52.07	44.34–49.93	47.99–70.67	42.73–47.62	38.09–53.93	44.24–50.19	44.84–46.42	45.78–51.70	38.1–75.1	45.08–48.77	45.57–49.66	48.58–52.36	37.59–46.96	43.31–48.77
Total Alkali (wt%)	0.57–4.09	0.72–3.56	2.79–7.08	0.64–4.49	0.05–3.71	3.59–5.81	3.09–3.57	1.27–4.39	1.75–9.82	2.45–5.08	1.11–2.90	2.61–4.15	0.05–1.18	0.62–2.50
Nb/Th	1.95–5.32	2.17–18.54	1.58–5.59	7.33–16.00	1.88–19.31	3.56–3.72	9.53–11.01	8.94–23.41	1.06–15.18	6.61–14.64	1.88–17.23	14.16–26.01	0.85–3.59	8.64–29.02
Zr/Nb	10.11–13.81	16.22–42.62	9.13–33.71	7.81–9.80	13.22–59.22	8.40–8.55	4.33–4.77	16.25–23.16	6.97–24.02	5.56–25.09	11.6–31.22	16.38–16.62	14.87–86.83	18.07–30.22
Zr/Y	3.66–5.43	2.03–5.34	2.81–11.77	3.21–4.52	1.07–4.27	4.62–4.78	3.40–3.71	2.25–3.05	2.60–7.29	2.31–6.49	2.02–3.77	2.37–2.53	1.30–20.89	2.04–3.16
Nb/Y	0.35–0.45	0.10–0.18	0.25–0.53	0.35–0.53	0.03–0.23	0.54–0.57	0.75–0.83	0.10–0.16	0.11–0.91	0.09–1.17	0.06–0.33	0.14–0.15	0.02–0.25	0.07–0.14
La/Sm	1.82–3.35	0.63–1.71	1.99–3.96	1.37–2.53	0.58–2.26	2.80–3.08	2.54–2.59	0.76–1.09	0.76–4.13	0.95–2.32	0.54–1.77	0.73–0.81	0.79–13.99	0.74–0.89
Gd/Yb	1.09–1.56	1.01–1.25	1.23–2.39	1.20–1.42	0.76–1.33	1.28–1.46	1.34–1.40	0.91–1.11	1.07–2.38	1.14–2.41	0.92–1.28	0.99–1.08	0.69–1.31	0.99–1.06
Eu/Eu*	0.83–1.06	0.87–1.07	0.68–1.45	0.85–1.05	0.54–1.46	0.75–1.07	0.98–1.01	0.89–1.22	0.64–1.16	1.00–1.36	0.95–1.17	1.00–1.05	0.48–1.50	0.96–1.07
Nb/Nb*	0.30–0.72	0.35–1.52	0.26–0.61	0.90–1.55	0.28–1.57	0.52–0.57	1.18–1.32	0.95–1.41	0.20–1.64	0.67–1.71	0.30–1.42	1.40–1.72	0.06–0.58	0.84–1.60
Ti/Ti*	0.67–1.07	0.57–0.97	0.24–0.87	0.90–1.10	0.60–1.07	0.72–0.80	0.84–1.36	0.76–1.07	0.29–1.24	0.88–1.08	0.87–1.02	1.13–1.58	0.31–0.89	0.89–1.14

The following sections describe the analytical methods used to collect the new data, how the data were screened for alteration and how each of the suites were classified.

3.1. Analytical procedures

3.1.0.1. Major and trace elements

Sample preparation and analysis for the new geochemical data presented in this paper was carried out at Cardiff University. After removal of weathered surfaces and veins, the samples were crushed using a steel jaw crusher and powdered in an agate planetary ball mill and ignited in a furnace at 900 °C for two hours to determine loss on ignition values.

Whole-rock major element, trace element and rare earth element (REE) data were obtained following Li metaborate fusion (see Minifie et al., 2013 for methodology). Major element and Sc abundances were determined using a JY Horiba Ultima 2 Inductively Coupled Plasma Optical Emission Spectrometer (ICP-OES). Other trace elements were analysed by a Thermo X Series 2 Inductively Coupled Plasma Mass Spectrometer (ICP-MS). International reference material JB-1A was run with each sample batch to constrain the accuracy and precision of the analyses. Relative standard deviations show precision of 1–5% for most major and trace elements for JB-1A. 2σ values encompass certified values for the vast majority of elements. Ranges of the whole-rock major element and trace element concentrations for the each of the CSLIP suites are presented in Table 2. Full analytical results including repeat runs of standard basalt JB-1A and granite NIM-G can be found in Electronic Appendix 3.

To augment the published radiogenic isotope data for the CSLIP, eighteen samples were selected for Nd-Hf isotopic analysis. The whole-rock geochemical data for those samples for which isotopic data were collected are presented in Table 3. The isotopic data were collected at the NERC Isotope Geosciences Laboratory in Keyworth, UK, using methods described in detail by Hastie et al. (2009). Lu-Hf data was analysed using a Thermo-Electron Neptune mass spectrometer, with a Cetac Aridus II desolvating nebuliser. Replicate analysis of the BCR-2 rock standard across the time of analysis gave a mean Lu concentration of 0.49 ppm ± 0.0001 ppm (1-sigma, n = 21) while replicate analysis of the JMC475 rock standard across the time of analysis gave a mean Hf concentration of 14.63 ppm ± 0.32 ppm (1-sigma, n = 21) and $^{176}Hf/^{177}Hf$ of 0.282150 ± 0.000005. Sm-Nd fractions were analysed on a Thermo Scientific Triton mass spectrometer. Repeat analysis of BCR-2 during the analysis period gave a mean Sm concentration of 6.34 ± 0.06 ppm (1-sigma, n = 7) while replicate analyses of the La Jolla standard gave a $^{143}Nd/^{144}Nd$ ratio of 0.511845 ± 0.000007 (10.4 ppm, 1-sigma).

3.2. Element mobility

As many of the CSLIP suites have experienced at least greenschist facies metamorphism, and samples typically show considerable alteration, the effects of secondary element remobilisation must be considered. A method used by Cann (1970) to assess element mobility is to construct bivariate diagrams with a generally accepted immobile element (e.g., Zr) on the horizontal axis and the element to be evaluated on the vertical axis. If both elements are immobile and incompatible during basaltic fractionation, the rock samples are derived from the same mantle source and are not subsequently contaminated, the data should yield good correlation coefficients and straight lines with gradients close to unity. If a large degree of scatter is visible on these diagrams then this may indicate that one of the elements was mobile and its concentration altered by secondary processes. Alternatively, a lack of correlation may be explained by the derivation of the igneous rocks in the same magmatic suite from a heterogeneous mantle source. Several of the CSLIP suites (Chukotat Group, Flaherty Formation, Molson dykes and Fox River Belt) appear to comprise two or more, geochemically distinct groups (Fig. 3; Table 4).

Table 3
Whole-rock geochemical data for the Circum-Superior LIP samples for which Nd-Hf isotopic data was collected.

	Hellancourt Formation		Flaherty Formation				Winnipegosis Belt		Molson dykes				Pickle Crow dyke	Hemlock Formation			Badwater Greenstone Belt
	MMLT07-28	MMLT07-41	MMF07-17	MMF07-14	MMF07-2	MMF07-7	MMW07-24	MMW07-4	MMM07-26	MMM07-20	MMM07-14	MMM07-17	MMPC07-2	MMH08-5	MMH08-7	MMH08-12	MMB08-6
(wt%)																	
SiO_2	46.47	48.81	43.62	44.51	44.60	44.51	48.77	44.82	46.73	47.37	49.41	48.59	48.58	52.55	48.92	50.13	49.50
TiO_2	1.42	0.89	2.03	2.32	2.20	2.29	1.10	0.54	0.60	0.67	1.01	1.52	1.84	1.74	1.01	1.81	1.20
Al_2O_3	15.25	14.00	13.70	13.76	13.70	13.35	14.24	8.09	10.62	10.62	13.63	14.33	12.51	12.34	13.68	14.02	13.35
Fe_2O_3	14.77	12.13	17.43	15.36	16.43	17.49	13.79	12.61	12.13	12.32	13.29	13.88	14.93	15.76	12.34	14.38	13.87
MnO	0.20	0.17	0.24	0.26	0.23	0.24	0.17	0.18	0.18	0.20	0.22	0.23	0.17	0.20	0.19	0.19	0.20
MgO	8.14	8.99	5.41	7.49	6.16	6.32	6.68	20.90	17.87	16.46	8.28	6.96	6.47	3.81	7.35	4.62	6.18
CaO	11.15	11.11	12.45	9.14	9.66	8.30	10.28	8.23	9.29	10.11	11.14	10.77	10.52	6.21	11.31	7.79	12.40
Na_2O	1.75	2.37	1.48	3.66	3.00	3.35	1.56	0.96	1.26	1.37	1.85	2.60	2.15	3.96	1.96	2.47	0.55
K_2O	0.13	0.07	0.12	0.24	0.25	0.55	0.06	0.08	0.06	0.12	0.09	0.27	0.46	1.67	0.13	2.40	0.02
P_2O_5	0.09	0.05	0.16	0.17	0.16	0.18	0.09	0.03	0.04	0.04	0.07	0.14	0.14	0.19	0.07	0.31	0.09
LOI	2.16	2.26	2.99	3.69	4.96	4.16	1.94	2.91	0.13	0.40	-0.22	0.44	0.91	1.46	2.04	1.92	2.37
Total	101.54	100.83	99.63	100.60	101.35	100.76	98.67	99.34	98.92	99.70	98.78	99.73	98.67	99.88	99.01	100.03	99.74
(ppm)																	
Sc	46.33	45.61	43.13	43.62	41.44	43.39	42.07	29.31	30.91	33.46	43.75	40.02	37.43	37.18	44.70	36.78	44.08
V	406.14	309.45	378.52	380.56	397.09	383.72	340.88	199.54	202.19	224.11	354.65	328.63	511.40	336.45	287.99	269.90	312.03
Cr	290.62	405.15	84.19	111.96	102.27	89.61	121.74	2113.16	954.07	1445.30	208.31	100.98	55.23	28.38	230.72	26.28	90.84
Co	55.94	48.27	61.03	55.99	59.87	59.97	50.27	83.84	56.51	66.21	49.09	56.50	48.80	46.52	44.50	51.13	48.64
Ni	155.22	144.77	103.28	135.88	388.20	57.42	116.42	705.48	319.07	428.00	126.64	70.31	61.56	84.62	84.40	31.35	51.66
Cu	131.53	104.70	–	–	–	–	–	87.09	–	–	–	–	158.08	–	–	–	–
Zn	84.49	47.90	101.84	59.38	84.61	83.45	202.37	57.07	166.33	229.22	204.71	165.57	86.06	135.92	91.77	110.66	104.17
Sr	178.91	129.47	435.26	246.62	191.07	181.85	122.60	49.08	62.63	66.65	84.49	167.29	124.26	174.64	116.14	242.04	394.71
Y	30.25	18.96	38.43	35.08	38.32	40.30	23.72	11.46	13.62	15.05	22.97	27.64	24.65	36.13	21.40	41.16	24.55
Zr	80.75	54.18	130.85	138.66	122.98	144.19	61.17	23.54	28.19	42.96	59.40	104.31	58.51	187.02	57.43	227.98	89.82
Nb	4.00	2.53	14.10	16.32	15.26	16.12	3.03	1.04	1.44	2.05	2.61	8.99	3.52	22.16	2.39	17.09	8.89
La	4.02	2.90	13.63	14.25	11.57	13.86	3.05	1.43	1.52	2.57	2.69	8.44	2.81	29.24	2.55	40.43	11.91
Ce	9.98	6.60	29.44	31.26	25.87	30.83	8.32	3.28	4.36	6.38	7.32	19.53	8.68	58.96	7.24	80.35	24.96
Pr	1.71	1.11	4.12	4.47	3.78	4.35	1.40	0.56	0.73	0.99	1.23	2.89	1.47	7.05	1.21	9.64	3.28
Nd	8.63	5.55	18.04	19.59	16.70	18.89	7.20	2.95	3.82	4.83	6.23	13.01	7.37	26.80	6.21	36.30	13.39
Sm	2.86	1.89	4.68	4.90	4.54	5.02	2.39	1.07	1.33	1.61	2.11	3.65	2.45	5.99	2.15	7.78	3.41
Eu	0.99	0.68	1.49	1.51	1.48	1.46	0.86	0.39	0.50	0.57	0.78	1.23	0.92	1.67	0.80	2.20	1.19
Gd	3.50	2.42	5.23	5.28	5.06	5.49	3.06	1.36	1.69	1.98	2.67	4.15	3.00	5.69	2.61	7.27	3.59
Tb	0.69	0.48	0.99	0.95	0.94	1.03	0.55	0.27	0.32	0.36	0.50	0.70	0.57	0.97	0.49	1.16	0.62
Dy	4.49	3.17	6.05	5.78	5.93	6.30	3.79	1.80	2.17	2.45	3.45	4.57	3.75	6.11	3.33	6.99	4.09
Ho	0.88	0.63	1.17	1.08	1.16	1.23	0.75	0.36	0.44	0.49	0.70	0.89	0.74	1.23	0.69	1.37	0.83
Er	2.66	1.93	3.52	3.21	3.41	3.62	2.23	1.09	1.25	1.42	2.08	2.57	2.24	3.53	2.01	3.82	2.39
Tm	0.43	0.31	0.54	0.49	0.54	0.57	0.36	0.16	0.20	0.23	0.33	0.40	0.34	0.57	0.33	0.59	0.37
Yb	2.77	2.02	3.53	3.15	3.50	3.75	2.39	1.10	1.30	1.48	2.18	2.69	2.29	3.45	2.01	3.59	2.28
Lu	0.43	0.33	0.55	0.48	0.54	0.59	0.36	0.17	0.20	0.23	0.34	0.41	0.36	0.56	0.33	0.57	0.37
Hf	1.81	1.16	3.12	3.18	2.89	3.52	1.56	0.56	0.67	1.10	1.31	2.52	1.51	4.56	1.39	5.50	2.26
Ta	0.28	0.18	0.79	0.93	0.84	0.89	0.19	0.07	0.09	0.13	0.16	0.52	0.19	1.18	0.18	0.89	0.51
Th	0.22	0.21	1.65	1.06	0.95	1.81	0.26	0.04	0.12	0.39	0.27	0.82	0.22	7.24	0.16	6.27	2.13
U	0.08	0.07	0.47	0.30	0.27	0.53	0.06	0.03	0.04	0.12	0.06	0.22	0.07	1.34	0.03	0.74	0.39

When such geochemically distinct groups have been accounted for, the bivariate diagrams of elements plotted against Zr (not shown) indicate that alteration has affected some of the major elements (e.g., K_2O, Na_2O and commonly CaO) in some suites. Additionally, and in keeping with other studies (e.g., Ciborowski et al., 2015; Pearce, 1996) alteration has particularly mobilised the Large Ion Lithophile Elements (LILE), while the High Field Strength Elements (HFSE) including the Rare Earth Elements (REE) have remained essentially immobile. Accordingly, this study will mostly focus on these more immobile elements and oxides.

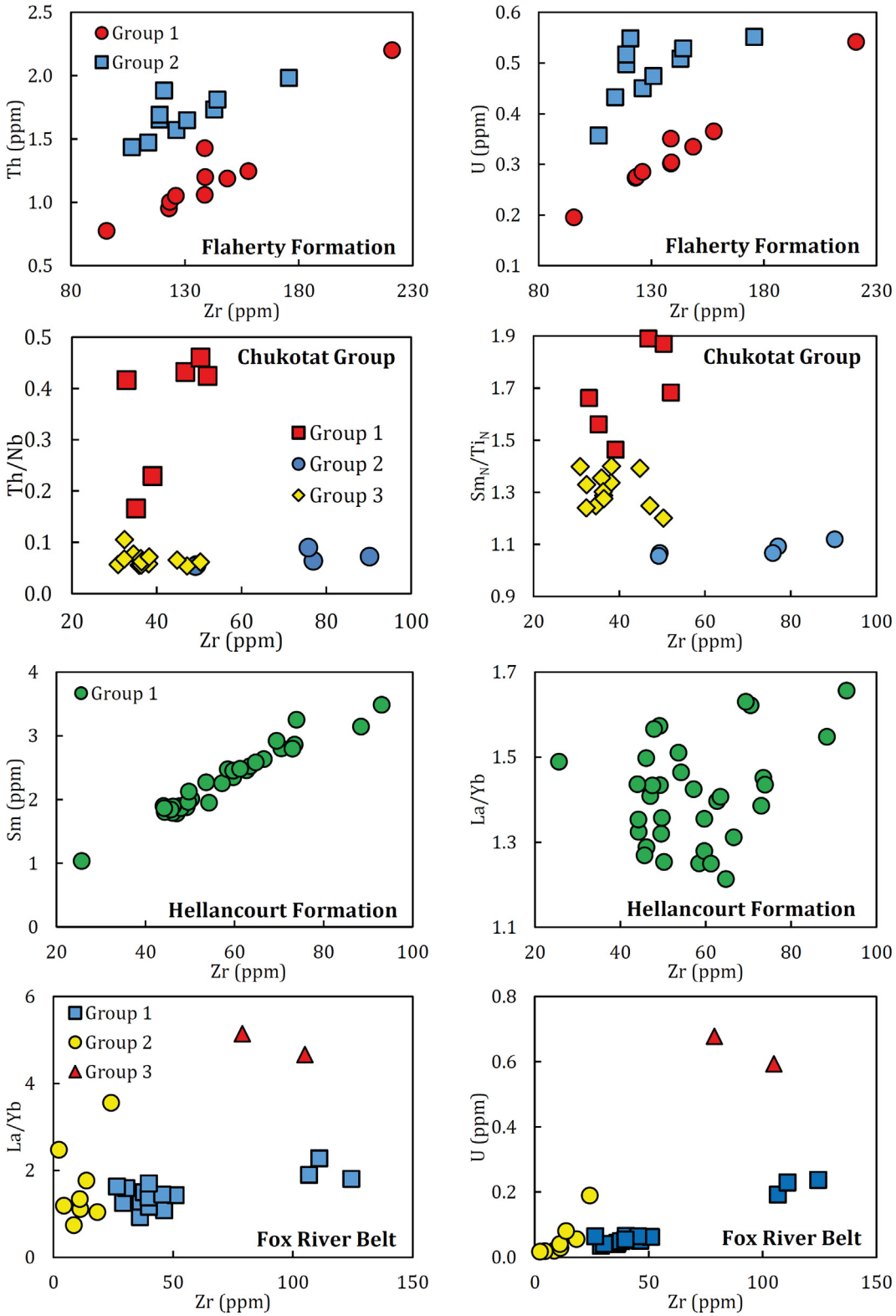

Fig. 3. Selection of bivariate diagrams which show the composite nature of several of the constituent suites of the Circum-Superior LIP.

Table 4
Table showing the chemical criteria used to subdivide composite formations of the Circum-Superior LIP.

Suite	Group	% of samples	Characteristics
Chukotat Group	1	25	Enrichments in LREE relative to HREE, negative Nb-Ta anomalies, negative Ti anomalies
	2	21	Enrichments in LREE relative to HREE, slightly positive Nb-Ta anomalies
	3	52	Depletions in LREE relative to HREE, positive Nb-Ta anomalies, negative Ti anomalies
Flaherty Formation	1	50	Enrichments in LREE relative to HREE, positive Nb-Ta anomalies
	2	50	Enrichments in LREE relative to HREE, no NB-Ta anomalies
Fox River Belt	1	60	Flat REE patterns and (Th/La)N ratios <1
	2	40	Enrichments in LREE relative to HREE and negative Nb-Ta anomalies
Molson dykes	1	27	Relatively flat REE patterns and negative Nb-Ta anomalies
	2	20	Enrichments in LREE relative to HREE and slightly positive Nb-Ta anomalies
	3	53	Depletions in LREE relative to HREE, slightly negative Ti anomalies
Hemlock Formation	1	22	Enrichments in LREE relative to HREE, slightly positive Nb-Ta anomalies
	2	11	Relatively flat REE patterns and Th/La ratios <1
	3	11	Enrichments in LREE relative to HREE, slightly negative Nb-Ta anomalies
	4	56	Enrichments in LREE relative to HREE, negative Nb-Ta anomalies, negative Ti anomalies

3.3. Classification

Since sub-solidus alteration of the Circum-Superior suites appears to have mobilised a number of major elements, particularly K_2O and Na_2O, the conventional alkali – silica classification diagram has not been used. As an alternative, the Zr/Ti vs. Nb/Y diagram (Pearce, 1996) has been used as it is based on immobile trace elements. On this diagram the majority of the CSLIP suites plot as overlapping clusters within the subalkaline basalt and basaltic andesite fields. Only the samples from the Thompson Nickel Belt differ from this general trend and instead plot predominantly as subalkaline andesites. A few samples from other localities classify as dacites, rhyolites and alkali rhyolites (Fig. 4).

3.4. Geochemical variation

A relatively common feature throughout the CSLIP is the presence of both high and low MgO rocks within individual segments (Fig. 5). The volcanic rocks of the Chukotat Group, Fox River Belt and Winnipegosis Belt and the Molson dykes all have large variations in MgO concentrations from 5.7 wt% to 26.7 wt%. The Hellancourt Formation and Flaherty Formation have fairly restricted ranges in MgO content of 6.0–9.9 wt% and 5.1–8.2 wt% respectively. The most felsic rocks of the CSLIP are found in the Lake Superior region where the overall range in MgO concentrations is from 0.5 to 10.8 wt%. Samples that have MgO > 12 wt% are referred to as picrites, however none of the rocks in this study can be called komatiites, as none possess spinifex-textured olivine (cf. Kerr and Arndt, 2001; Arndt, 2003).

A trace element signature similar to that of oceanic plateaus, such as the Ontong Java Plateau, is common throughout a large portion of the CSLIP. This signature has essentially flat REE and multi-element normalised profiles with the exception of Th which is slightly depleted with respect to the other elements (Fig. 6). Such a signature is present in the Chukotat Group, Fox River Belt, Winnipegosis Belt, Molson dykes, Pickle Crow dyke, Labrador Trough and Group 1 of the Hemlock Formation. The vast majority of samples from these areas plot within the field of 'oceanic plateau basalts' on trace element ratio:ratio plots such as the Zr/Nb- Nb-Th and Nb/Y-Zr/Y diagrams (Fig. 7a and b).

Samples with multi-element profiles having negative Nb-Ta anomalies are also present in many of the segments of the CSLIP and plot as overlapping clusters on tectonic discrimination diagrams within fields defined by volcanic-arc basalts (Fig. 7a and b). All of the Thompson Nickel Belt samples have large negative Nb-Ta anomalies with Nb/Nb*[1] values of 0.08–0.62 while the majority of samples from the Lake Superior region (Gunflint Formation, Badwater Greenstone, Emperor Volcanic Complex, and Group 2 of the Hemlock Formation) also have strongly negative Nb-Ta anomalies in their multi-element-normalised profiles. A few of the samples of the Molson dykes and Chukotat Group and most of the intrusive samples from the Fox River Belt also contain negative Nb-Ta anomalies. No such anomalies are present in the Flaherty Formation, Winnipegosis Belt, Pickle Crow dyke or Hellancourt Formation. Primitive Mantle-normalised trace element diagrams showing the varying subgroups of each of the CSLIP suites are showing in Electronic Appendix 4.

The two subgroups which make up the Flaherty Formation basalts have trace element signatures which are somewhat different to the rest of the CSLIP, in that both groups are more enriched in Th-Nb-Ta-LREEs relative to the incompatible elements than the other CSLIP samples with an oceanic-plateau-like signature. The low MgO Group 3 samples of the Molson dykes and Group 3 of the Hemlock Formation are also similarly enriched in the more incompatible elements. The two groups of the Flaherty Formation are best distinguished on the basis of Nb-Ta anomalies relative to Th and La. One group has positive Nb-Ta anomalies (similar to OIB-like signatures) while the other group has no Nb-Ta anomalies. Positive Nb-Ta anomalies are also found in three samples away of Hudson Bay; one from the Molson dykes, one from the Hemlock Formation and one from the Kiernan sills.

One interesting feature of some of the trace element signatures of the Chukotat Group, Fox River Belt and Hellancourt Formation is the presence of negative Ti anomalies (Ti/Ti*[2]) with no concomitant negative Nb-Ta anomalies. These negative Ti anomalies generally occur in the higher MgO samples and are absent in the lower MgO samples.

Further compositional differences exist between the segments of the CSLIP in terms of HREE patterns (and so $(Gd/Yb)_N$ ratios). Samples from the Chukotat Group, Fox River Belt, Winnipegosis Belt, Groups 1 and 2 of the Molson dykes, Pickle Crow dyke, Group 1 of the Hemlock Formation, Hellancourt Formation and some from the Thompson Nickel Belt have flat HREE patterns and $(Gd/Yb)_N$ ratios close to unity. Samples from the Flaherty Formation, Haig sill, Group 3 of the Molson dykes, Lake Superior region (except Group 1 of the Hemlock Formation) and some from the Thompson Nickel Belt have more negatively-sloping HREE patterns and $(Gd/Yb)_N$ ratios greater than 1.2 (Fig. 7c).

3.5. Isotopic data

Eighteen samples were selected for Nd-Hf isotopic analysis. Hf isotope ratios were successfully determined for all eighteen sam-

[1] $\frac{Ti}{Ti^*} = \frac{Ti_N}{0.5\times(Sm_N+Gd_N)}$

[2] $\frac{Nb}{Nb^*} = \frac{Nb_N}{0.5\times(Th_N+La_N)}$

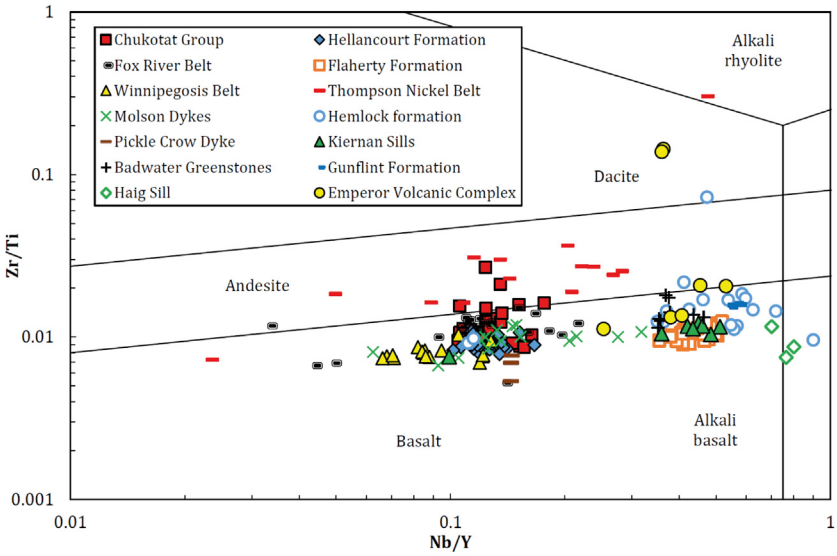

Fig. 4. Zr/Ti vs Nb/Yb classification diagram (after Pearce, 1996) for the Circum-Superior LIP suites.

ples. However, four samples failed to run on the mass spectrometer for Nd isotopes (Table 5).

The Badwater Greenstone sample and three samples from Groups 2 and 3 of the Hemlock Formation have εNd_i values ranging from +0.84 to −7.77. The εNd_i values for the Pickle Crow dyke and the Winnipegosis Belt Group 2 samples are +5.29 and +2.34 respectively. The other samples have εNd_i values that fall between those of the Pickle Crow dyke and Winnipegosis Belt Group 2 samples.

The Badwater Greenstone and Hemlock Formation Groups 2 and 3 samples have εHf_i values ranging between +0.81 and −6.09. The εHf_i values of the Molson dykes and Flaherty Formation range between +2.27 and +7.48 while the range for the Pickle Crow dyke, Hemlock Formation Group 1 and Winnipegosis Belt samples is from +9.86 to +14.03. The Hellancourt Formation samples have high εHf_i values of +28.18 and +29.44.

4. Discussion

4.1. Fractional crystallisation

A number of CSLIP suites are made up of several, compositional distinct subgroups (Fig. 2). This section will assess whether the subgroups of each suite are related to each other by fractional crystallisation (FC) or assimilation fractional crystallisation (AFC). To do this, MELTS_Excel (Gualda and Ghiorso, 2015) has been used to model the petrogenetic evolution of the Chukotat Group, which is an ideal model system for assessing these processes across the entire CSLIP, as it is made up of three compositionally disparate groups which span the range of trace element signatures found throughout the CSLIP.

MELTS_Excel (MELTS) is thermodynamic modelling software for investigating crystallisation and melting in natural magmatic systems (Gualda and Ghiorso, 2015). MELTS_Excel can calculate the proportions and compositions of solid and liquid phases in equilibrium assemblages by utilising thousands of experimentally-determined compositions of silicate liquids. The software can be applied to both hydrous and anhydrous magmatic systems over a temperature range of ~500–2000 °C and pressures <2 GPa.

The major element geochemical trends for the Chukotat Group have been modelled using four different MELTS fractional crystallisation scenarios: *Model 1*: 1 kbar (anhydrous); *Model 2*: 1 kbar (1% H_2O); *Model 3*: 5 kbar (anhydrous); Model 4: 10 kbar (anhydrous). All models use a quartz-fayalite- magnetite (QFM) oxygen buffer and calculate the composition of the residual magma at 10% crystallisation intervals. This modelling used the most primitive (highest MgO sample) from the Chukotat group (MMC08-14: 19.88 wt% MgO), which though unlikely to be a true primary magma, represents the closest approximation.

The major element trends of the Chukotat group rocks are variably replicated by both model 1 and model 2. For example, the variation of MnO, P_2O_5 and Al_2O_3 within the Chukotat group are best explained by fractionation of a magma similar in composition to MMC08-14 at 1 kbar under anhydrous conditions, while the variation in Fe_2O_3, TiO_2 and CaO form trends intermediate between models 1 and 2 (Fig 8). Therefore, the most likely scenario for the evolution of the Chukotat group magmas is one whereby a parent magma, similar in composition to MMC08-14, fractionated an assemblage of olivine, clinopyroxene, spinel and plagioclase in a shallow crustal chamber (~1 kbar) in the presence of a small amount (<1 wt%) of water.

The model which best predicts the anhydrous major element geochemical trends observed in each of the suites has been further tested using incompatible trace elements. This is achieved by using the mineral assemblages predicted to form by MELTS during crystallisation and the empirically derived mineral/melt partition coefficients of Bédard (2001) – see Electronic Appendix 5. These factors are applied to models which simulate both the Fractional Crystallisation (FC) and Assimilation-Fractional Crystallisation (AFC) of the parent magmas to each of the CSLIP suites. In the case of the latter, the evolution of the parent magmas is modelled using an upper crust contaminant (Rudnick and Gao, 2003) and assimilation/fractionation ratios (r) between 0.1 and 0.5.

For the Chukotat group rocks (Fig. 9), this modelling shows that AFC involving crustal contaminants is capable of replicating the LREE/HREE enrichment, and the increasingly negative Nb and Ti anomalies observed in the Chukotat group 1 samples. Interestingly, some of the most primitive Chukotat group 1 samples are those which have some of the most negative Nb-Ta anomalies, while more evolved samples have less negative Nb-Ta anomalies. This feature cannot be replicated by the AFC model, which may suggest that either a number of different contaminants were involved in the evolution of the group, or that a process similar to Assimilation during Turbulent Ascent (ATA) contaminated the hotter, more primitive magmas in thin dyke and sill-like magma chambers, while the cooler, more evolved magmas did not assimilate as much

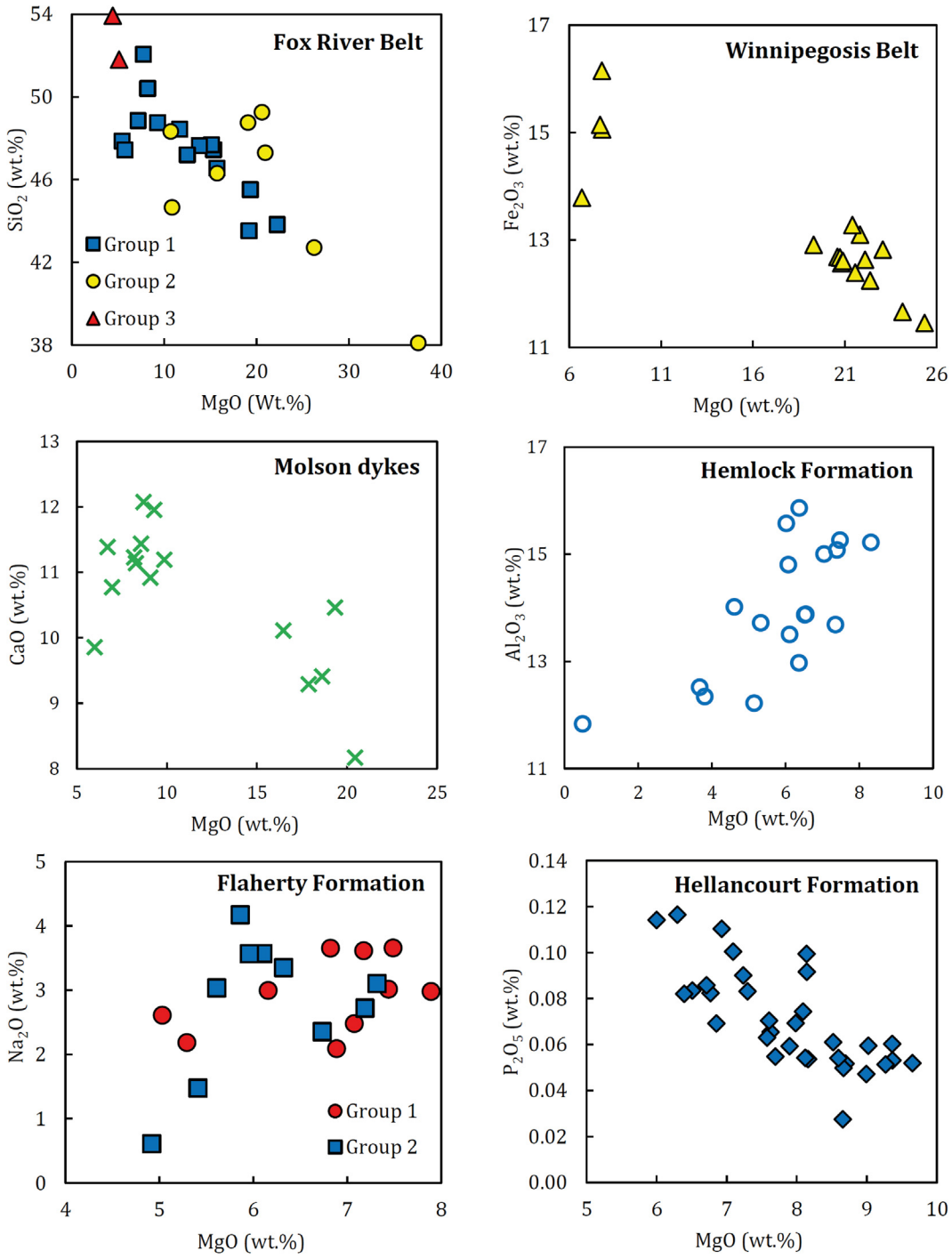

Fig. 5. Bivariate diagrams showing the major element variation for selected Circum-Superior LIP suites.

crust (e.g., Huppert and Sparks, 1985; Kerr et al., 1995). Conversely, the largely constant REE ratios and insignificant Nb anomalies displayed by groups 2 and 3 are replicated by the FC model. None of the models described above are capable of predicting the difference in magnitude in Ti anomalies which distinguishes the group 2 Chukotat rocks from the other two. Instead, this feature is potentially due to group 2 samples having a different mantle source than the group 3 rocks which themselves are characterised by significantly negative Ti anomalies. This is explored further in Section 4.5.

Similar modelling was carried out for the other CSLIP suites for which more ≥10 samples were collected (Electronic Appendix 6). This modelling is summarised in Table 6. In summary, the major and trace element trends of the CSLIP rocks record evidence of the primary magmas of the province having fractionated in relatively shallow-level magma chambers (<5 kbar pressure) within the crust. While some of the magmas underwent little crustal contamination other magmas were clearly contaminated, both during fractionation, and during ascent with minimal associated fractionation.

4.2. Magma genesis

As previously noted, the most primitive sample from each suite does not necessarily equate to the primary magma of that suite

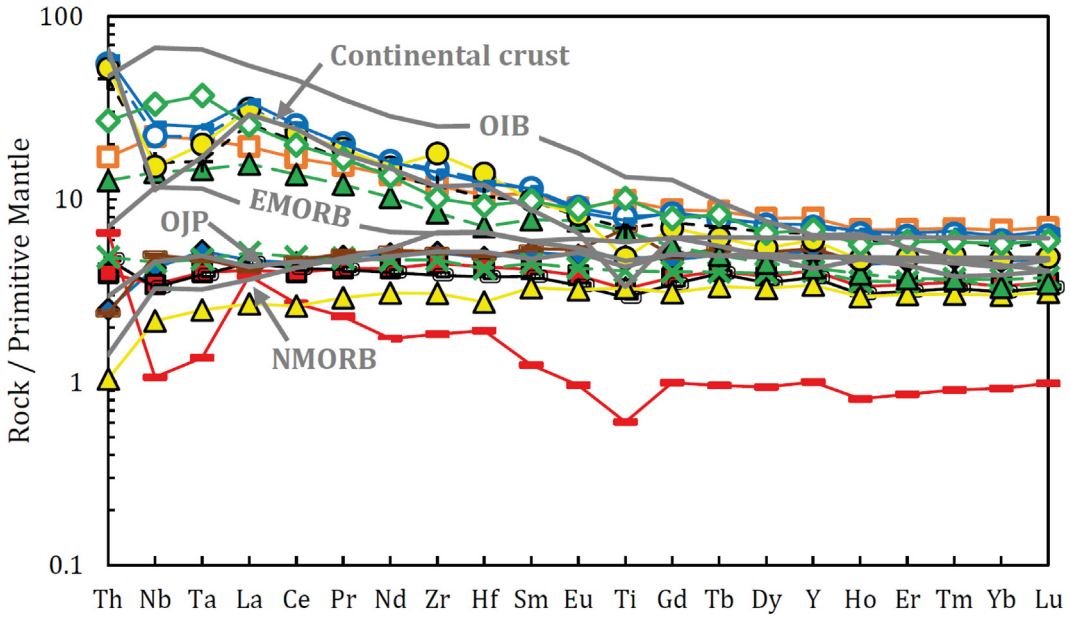

Fig. 6. Primitive-Mantle normalised trace element diagram of the average composition of each of the constituent suites of the Circum-Superior LIP. NMORB, EMORB and OIB compositions taken from Sun and McDonough (1989). Ontong Java Plateau (OJP) composition from average of 61 samples from Fitton and Godard (2004). Continental crust composition taken from average continental crust composition of Rudnick and Fountain (1995). Normalising factors taken from McDonough and Sun (1995). Symbols as in Fig. 4.

given the potential for post-melt modification of the primary magma. Assessment of the mantle source and calculation of the source melting temperature, along with the extent and depth of melting of the primary magmas of constituent suites of the CSLIP, relies on being able to accurately model the petrogenesis of these primary magmas. Herzberg and Asimow (2015) have developed the PRIMELT3 software which models both batch and accumulated fractional melting using hybrid forward and inverse models to incrementally add or subtract olivine from an evolved lava composition until a melt fraction is generated which is capable of: (a) being formed by partial melting of mantle peridotite, and; (b) replicates the major element composition of the starting magma through fractionation or accumulation of olivine. Through this modelling, PRIMELT can also calculate the degree of partial melting and mantle potential temperature (T_P), required to generate a primary magma from a more-evolved magma composition.

For all samples studied, $Fe^{2+}/\Sigma Fe$ and Fe_2O_3/TiO_2 ratios in the mantle peridotite were kept at 0.9 and 0.5 respectively. All of the samples containing >7.5 wt% MgO (n = 115) from the margins of intrusions and basalt provinces which make up the CSLIP were assessed using PRIMELT. The program was able to calculate primary magma compositions for the Hellancourt Formation, Chukotat Group, Fox River Belt, Winnipegosis Belt, Molson dykes, Badwater Greenstone volcanics and Emperor Volcanic Complex based on melting of a mantle peridotite similar in composition to Kettle River sample KR-4003 (Herzberg and O'Hara, 2002). In total, PRIMELT was able to calculate primary magma compositions for 17 samples from the CSLIP and these results are summarised in Table 7.

4.3. The case for a thermal plume?

Calculated primary magmas for Chukotat group samples contain (on average) 18.7 wt.% MgO. These magmas are in equilibrium with olivine of composition ~$Fo_{91.7}$ and would require ~33% melting of mantle peridotite with an average mantle T_p of 1530 °C using the calculation method of Herzberg and Asimow (2015) (i.e., the temperature the mantle would reach if brought to the surface adiabatically without melting (McKenzie and Bickle, 1988)). PRIMELT was also able to calculate primary magma compositions for five of the Winnipegosis samples. These primary magmas contain (on average) 23.1 wt% MgO, are in equilibrium with olivine of composition ~$Fo_{93.0}$ and also require ~33% melting of peridotite with an average mantle T_p of 1673 °C. Similar MgO contents, olivine compositions and degrees of melting were successfully calculated by PRIMELT for samples from the Fox River Belt, the Molson dykes, the Emperor Volcanic Complex (Table 7).

Mantle plumes are characterised by thermal anomalies in the upper mantle that are several hundreds of degrees hotter than ambient mantle (e.g., Wolfe et al., 1997; Cao et al., 2011). The temperature of the mantle source is therefore a key line of evidence in assessing the validity of a mantle plume origin for the CSLIP (advocated by Buchan et al. (2003) and Desharnais (2005)) as opposed to a model of passive upwelling of asthenospheric upper mantle along thinned continental margins (French et al., 2008; Heaman et al., 2009). Calculation of mantle potential temperatures (T_p), that can then be compared to secular cooling estimates of upper (ambient) mantle temperatures at a particular time (in the case of the CSLIP, 1.88 Ga), to assess the likelihood of a hot mantle plume source.

The average T_p calculated for the CSLIP suites by PRIMELT is 1562 °C which masks a significant range between the a sample from the Winnipegosis Belt (MMW07-9; T_P = 1686 °C) and a sample of the Emperor Volcanic Complex (MME08-1; T_P = 1438 °C) (Table 7). The total uncertainty in T_P calculated by PRIMELT is ±60 °C (2σ) (Herzberg and Asimow, 2015). The T_p of the primary magmas by PRIMELT are very similar to the T_p calculated using the method of Lee et al. (2009) – see Section 4.4 and Table 8.

Mantle cooling models suggest that the Paleoproterozoic mantle was significantly hotter than the modern mantle. Richter (1988) proposed a cooling model where the starting temperature of the upper mantle at 4.5 Ga was ~2500 °C, cooling at a continuously decreasing rate to reach a present day value of 1350 °C. In the first of several, more recent studies, Korenaga (2008) proposed that the mantle initially increased in temperature from ~1650 °C at 4.5 Ga to ~1700 °C at 3.6 Ga, followed by an increasingly rapid

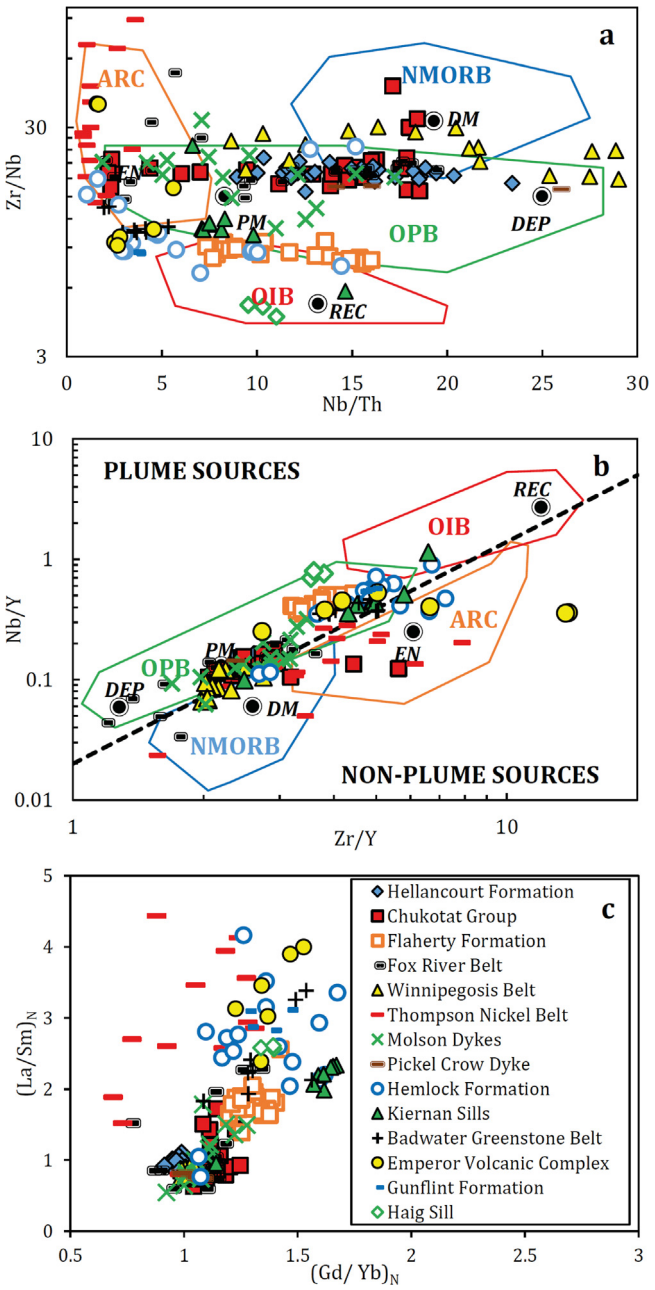

Fig. 7. Zr/Nb vs Nb/Th (a), Nb/Y vs Zr/Y (b) and (La/Sm)N vs (Gd/Yb)N (c) for the Circum-Superior LIP suites. Field boundaries and end-member compositions from Condie (2005). PM – primitive mantle, DM – shallow depleted mantle, ARC – arc-related basalts, NMORB – normal mid-ocean ridge basalts, OPB – oceanic plateau basalt, OIB – ocean island basalt, DEP – deep depleted mantle, REC – recycled component. Primitive Mantle-normalisation factors from McDonough and Sun (1995).

cooling rate to the present-day value of 1350 °C. Subsequent work by Davies (2009) challenged the low Urey ratio used by Korenaga (2008) and instead suggested a secular cooling model more consistent with that of Richter (1988) characterised by a constantly decreasing temperature from an initial upper mantle temperature of 1800 °C at 4.5 Ga to reach a modern day temperature of 1300 °C. In contrast, Herzberg et al. (2010) proposed a model similar to that of Korenaga (2008) whereby an initial warming of the mantle during the Hadean and Archaean led to a mantle temperature maximum occurring at 2.5 – 3.0 Ga before cooling to reach a modern day temperature of ~1350 °C.

These various secular cooling models are shown on Fig. 10 along with the calculated T_p [using both PRIMELT and the method of Lee et al. (2009)] of the CSLIP suites. All of the CSLIP samples, bar the single sample from the Emperor Volcanic complex are significantly hotter (>120 °C) than the upper mantle at 1.88 Ga as proposed by Davies (2009) and >50 °C hotter than that proposed by Richter (1988), but lower than that modelled by Korenaga (2008) and Herzberg et al. (2010). In fact, only samples from the Winnipegosis Belt record T_p greater than Korenaga's (2008) estimate of the upper mantle at 1.88 Ga.

The most recent cooling models from Herzberg et al. (2010), which are similar to that published by Korenaga (2008), and Davies (2009), differ hugely (~300 °C) in their estimates of the temperature of the upper mantle at 1.88 Ga. This difference is the product of the different model parameters used by the different authors: Davies (2009) contends that some of the assumptions made by Korenaga (2008) regarding plate thickness, Urey ratio (mantle heat production divided by heat loss) and plate curvature at subduction zones appear to be incorrect (Davies, 2009; Karato, 2010), while conversely, Herzberg et al. (2010) argues that the Urey ratio employed in the model of Davies (2009) is too high and in conflict with cosmochemical constraints on the amount of radiogenic elements in the mantle.

Other studies have estimated the T_p of ambient upper mantle various times in the Precambrian. Galer and Mezger (1998) calculated the T_p of the upper mantle at ~3 Ga to be 170 °C hotter than today. Their model suggests upper mantle cooling rates of ~57 °C/Ga which constrains the T_p of the upper mantle at 1880 Ma to ~1407 °C –between the estimates of Davies (2009) and Richter (1988). Ohta et al. (1996) and Komiya et al. (2004) identified MORB rocks within the ~3.3 Ga greenstones in the Cleaverville area of Western Australia and the ~3.8 Ga Isua greenstones of Greenland respectively and calculated the T_p of the upper mantle in the Archaean to be ~1480 °C. Based on dykes in west Greenland and northeast Canada, Mayborn and Lesher (2004) determined the T_p of upper mantle at 2.04 Ga to be 1420 °C. All of these estimates point to a significantly cooler upper mantle than is suggested by the models presented by Korenaga (2008) and Herzberg et al. (2010) and so support an anomalously hot mantle source for most of the suites that comprise the CSLIP. We therefore contend that it is most likely that the CSLIP has been derived from a thermal anomaly (mantle plume) in the upper mantle at ~1.88 Ga.

4.4. Depth of melting

During melting, major element ratios such as SiO_2/MgO, CaO/Al_2O_3, and Al_2O_3/TiO_2 are sensitive to pressure and temperature and can be used to assess where melting occurs in the mantle (e.g., Herzberg, 1995; Herzberg and Zhang, 1996; Walter, 1998; Arndt, 2003). One particular thermobarometer, FractionatePT (Lee et al., 2009) is based on SiO_2 contents of primary magmas and is applicable to melts derived from peridotitic sources. This makes it ideal for assessing the depth of melting for the individual primary magmas of the CSLIP discussed in Section 4.3.

Using FractionatePT (Lee et al., 2009) it can be calculated that the primary magmas of the CSLIP were generated at a range of pressures from 1.72 to 5.82 GPa (Fig. 11 and Table 8). Further, within some of the individual suites, melting occurred over a significant range of pressures; for example in the Winnipegosis Belt the calculated pressure of melting ranges from 3.94 to 5.82 GPa. These pressures (depths) of melting of the CSLIP are all within the garnet stability field. However, the Gd_N/Yb_N ratios of all of the suites for which primary magmas could be calculated are all very close (0.91–1.11) to unity (Fig. 7c), suggesting a shallow spinel-bearing source. This paradox can be reconciled on the basis of garnet peridotite melting experiments. Walter (1998) showed

Table 5
New Sm-Nd and Lu-Hf isotope data for representative Circum-Superior LIP suites. Initial values (i) calculated for when t = 1880 Ma.

Sample	Nd	Sm	$^{147}Sm/^{144}Nd$	$^{143}Nd/^{144}Nd$	εNd_i	Lu	Hf	$^{176}Lu/^{177}Hf$	$^{176}Hf/^{177}Hf$	εHf_i
Molson dykes										
MMM07-14	4.88	1.82	–	–	–	0.37	1.84	0.0287	0.282824	7.5
MMM07-17	11.41	3.24	–	–	–	0.40	2.71	0.0211	0.282542	7.1
MMM07-26	4.39	1.53	–	–	–	0.25	1.19	0.0299	0.282824	6.0
MMM07-20	4.78	1.60	0.2021	0.512853	2.9	0.24	1.28	0.0265	0.282719	6.6
Hemlock formation										
MMH08-5	14.85	3.50	0.1425	0.511698	-5.3	0.49	4.32	0.0161	0.282087	−2.7
MMH08-20	20.40	4.82	0.1429	0.512015	0.8	0.32	2.39	0.0192	0.282294	0.8
MMH08-12	31.53	6.53	0.1252	0.511357	−7.8	0.47	4.61	0.0144	0.281931	−6.1
MMH08-7	4.32	1.53	0.2133	0.513013	3.3	0.24	0.79	0.0424	0.283495	14.0
Winnipegosis belt										
MMW07-24	5.72	2.03	0.2151	0.512985	2.3	0.31	1.27	0.0352	0.283198	12.6
MMW07-4	3.10	1.12	–	–	–	0.18	0.93	0.0276	0.282851	9.9
Hellancourt formation										
MMLT07-28	8.38	2.82	0.2037	0.512914	3.7	0.35	0.74	0.0675	0.284826	29.4
MMLT07-41	5.11	1.72	0.2034	0.512931	4.1	0.25	0.55	0.0633	0.284640	28.2
Pickle Crow dyke										
MMPC07-2	4.65	1.68	0.2181	0.513173	5.3	0.36	2.14	0.0239	0.282735	10.5
Flaherty formation										
MMF07-17	11.36	3.30	0.1758	0.512512	2.6	0.51	3.69	0.0195	0.282406	4.4
MMF07-14	7.61	2.40	0.1905	0.512701	2.7	0.38	3.71	0.0144	0.282262	5.8
MMF07-2	6.57	2.10	0.1934	0.512811	4.2	0.45	3.43	0.0185	0.282421	6.2
MMF07-7	6.85	2.21	0.1952	0.512741	2.4	0.46	3.63	0.0181	0.282297	2.3
Badwater greenstone belt										
MMB08-6	12.19	3.05	0.1512	0.511979	−1.9	0.30	1.70	0.0249	0.282465	−0.4

that at lower pressures (3 GPa) garnet remained in the residue until ~10% melting and at high pressures (>7 GPa) ~65% melting is required to exhaust all the garnet. The >30% melting required to produce the CSLIP primary magmas would therefore probably be enough to melt out most of the garnet in the source at pressures recorded in Table 8.

Seismic studies have suggested that the thickness of the cratonic root of the Superior Province may be ~300 km (e.g., van der Lee and Nolet, 1997; Sol et al., 2002). The major element chemistry of the primary magmas from the Chukotat Group, Fox River Belt, Winnipegosis Belt and Molson dykes indicates that melting in these regions occurred at pressures ranging from 1.72–5.82 GPa which equates to a range in the depth of melting of ~64–162 km. Therefore, large scale melting may not have occurred under the thickest lithosphere of the Superior Province, but instead could be associated with a plume that spread along the base of the lithosphere to reach areas of thinner lithosphere such in the Thompson region, Chukotat and Hellencourt regions (see further discussion below).

4.5. Mantle source composition

4.5.1. Isotopic considerations

Nd and Hf isotope systematics are generally little affected by elemental mobility and are therefore appropriate for studying the petrogenesis of ancient and/or altered igneous rocks such as the CSLIP. Hf-Nd isotopic compositions of the CSLIP samples are shown in Fig. 12 and are compared to the results of previous studies on the Chukotat Group (Blichert-Toft and Arndt, 1999; Vervoort and Blichert-Toft, 1999) and Fox River Belt (Desharnais, 2005). Generally, the samples analysed in this study are similar to results from these previous studies, which may indicate a common mantle source for the majority of the Circum-Superior magmatism. Notable exceptions to this are some of the Hemlock Formation, which plot on a linear array extending from the majority of the Circum-Superior LIP samples towards Archaean crustal components. This isotopic trend is consistent with the Hemlock Formation magmas having been contaminated by crustal material.

The most radiogenic Hf isotopic signature is seen in the Hellancourt Formation (εHf_i = +28 to +30) despite the Nd isotopic signature of these samples being the same as that of the Chukotat Group. While rare in the mantle, extremely positive εHf values have been reported by Nebel et al. (2013, 2014) in Archaean komatiites from the Yilgarn craton which they interpreted to be derived from partial melting of an ancient, melt-depleted mantle reservoir. Nebel et al. (2013, 2014) suggest that such a reservoir – termed the Early Refractory Reservoir (ERR) – could be the residue from the formation of the earliest Hadean terrestrial crust and could have been remelted by hot, upwelling plumes to ultimately produce mafic lavas characterised by superchondritic initial $^{176}Hf/^{177}Hf$ signatures. High εHfi values (up to + 76) have also been recorded in peridotite mantle xenoliths from Hawaii (Salters and Zindler, 1995; Bizimis et al., 2007) and these have been proposed to represent ancient (>2 Ga) depleted mantle lithosphere caught up in the Hawaiian plume (Bizimis et al., 2007).

4.5.1.1. Trace element considerations. The trace element geochemistry of the CSLIP suites is varied (Fig. 6). Several of the suites in the CSLIP have geochemical signatures characterised by depletions in the most incompatible elements and relative enrichments in the HREE (e.g., Hellancourt Formation, Winnipegosis Belt, Fox River Belt volcanics) (Signature 1; Fig. 13a). Such signatures have been interpreted elsewhere as being derived through partial melting of a depleted (upper) mantle source (e.g., Workman and Hart, 2005).

Signature 2 is typified by the Fox River Intrusions, Thompson Nickel Belt, and Gunflint Formation and is characterised by enrichments in the most incompatible elements and significantly negative Nb-Ta and Ti anomalies (Fig. 13b). Although such signatures can be attributed to the petrogenetic processes in volcanic arc settings (e.g., Pearce and Peate, 1995), our modelling in Section 4.1 suggests that these signatures are more likely to be due to the contamination of mantle melts by continental crust during fractionation.

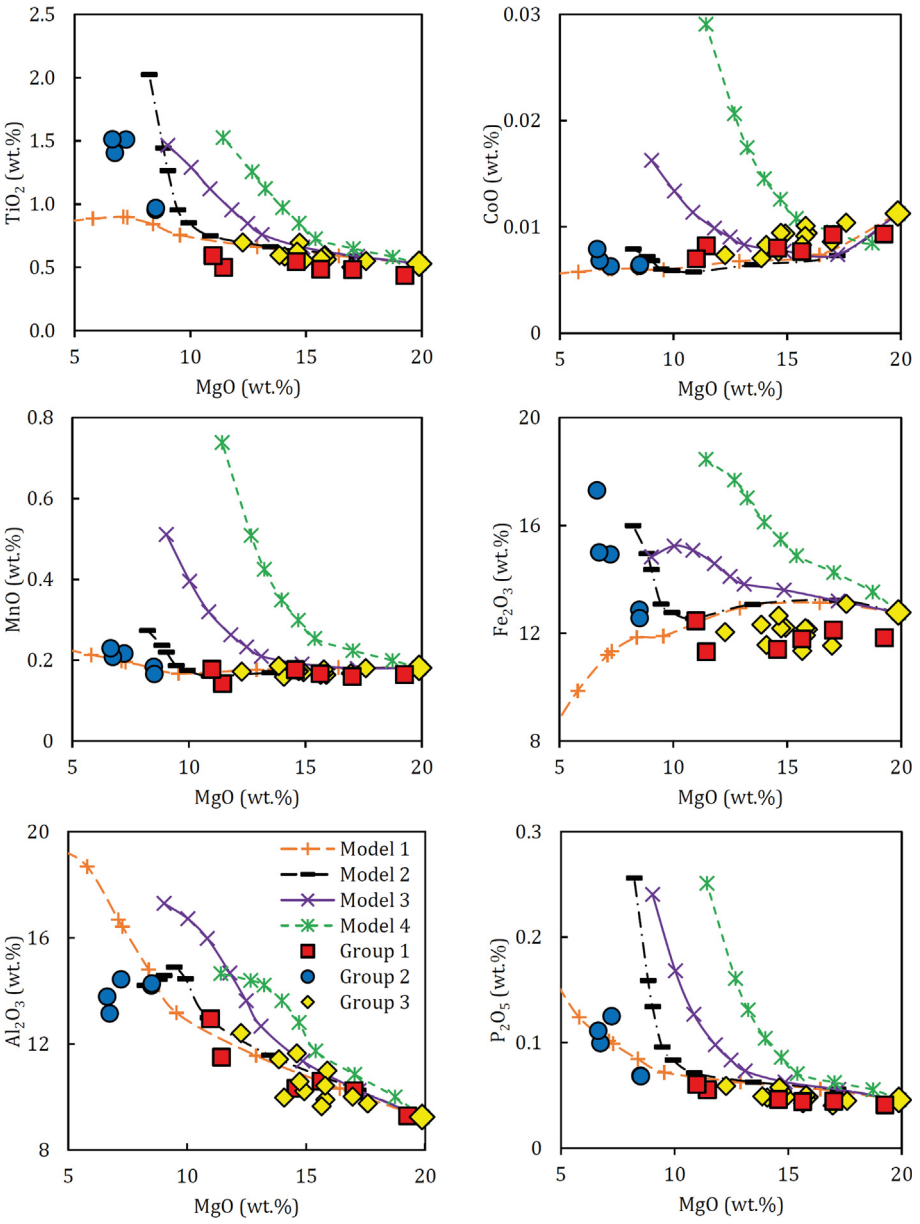

Fig. 8. Bivariate diagrams showing the major element evolution of the Chukotat Group parental magma (MMC08-14) during fractional crystallisation (FC). Markers indicate increments of 10% crystallisation. See text for description of models.

Signature 3 is arguably the most enigmatic in the CSLIP and is exemplified by Group 3 of the Chukotat Group and Group 2 of the Fox River belt. Unlike other suites which record a negative Ti anomaly (e.g., Gunflint Formation, Thomspon Nickel Belt), this signature is not associated with a negative Nb-Ta anomaly (Fig. 13c), and so cannot be easily explained by contamination of melts with continental material.

Signature 4 is typified by the Flaherty Group samples and these are enriched in the most incompatible elements relative to the HREE and have markedly positive Nb-Ta anomalies (Fig. 13d). These signatures are similar to modern day OIBs.

Samples from the Chukotat Group, Fox River Volcanics, Winnipegosis Belt, Emperor Volcanic Complex and Molson dykes (for which primary magmas were calculated by PRIMELT) span these geochemical groups (Fig. 13) and provide a subset of analyses which reflect the compositional variation in the CSLIP as a whole.

To investigate the potential mantle sources of these suites, three mantle reservoirs were modelled: Depleted MORB Mantle (DMM; Workman and Hart, 2005), Primitive Mantle (PM; McDonough and Sun, 1995), and Enriched Mantle 1 (EM1; Chauvel et al., 1992). Although using these modern reservoirs for Proterozoic rocks is somewhat speculative, they nevertheless can be used to characterise the broad nature of the mantle source regions of the CSLIP. The ~30% partial melting needed to form the CSLIP primary magmas (Table 7) is modelled using batch melting of spinel lherzolites (Johnson et al., 1990) to simulate the flat HREE patterns in the CSLIP (Fig. 6).

These calculated melts were then modelled for the fractional crystallisation of olivine (to the extent predicted by PRIMELT) using the melt-mineral partition coefficients in Table 7 and Electronic Appendix 5. This modelling shows that partial melting of DMM-like and EM1-like sources (or perhaps a hybrid source) could feasibly produce the 'Signature 1' trace element signature observed in the Winnipegosis belt rocks (Fig. 13a).

Modelling of these reservoirs is unable to replicate the 'Signature 2' type trace element patterns (characterised by negative

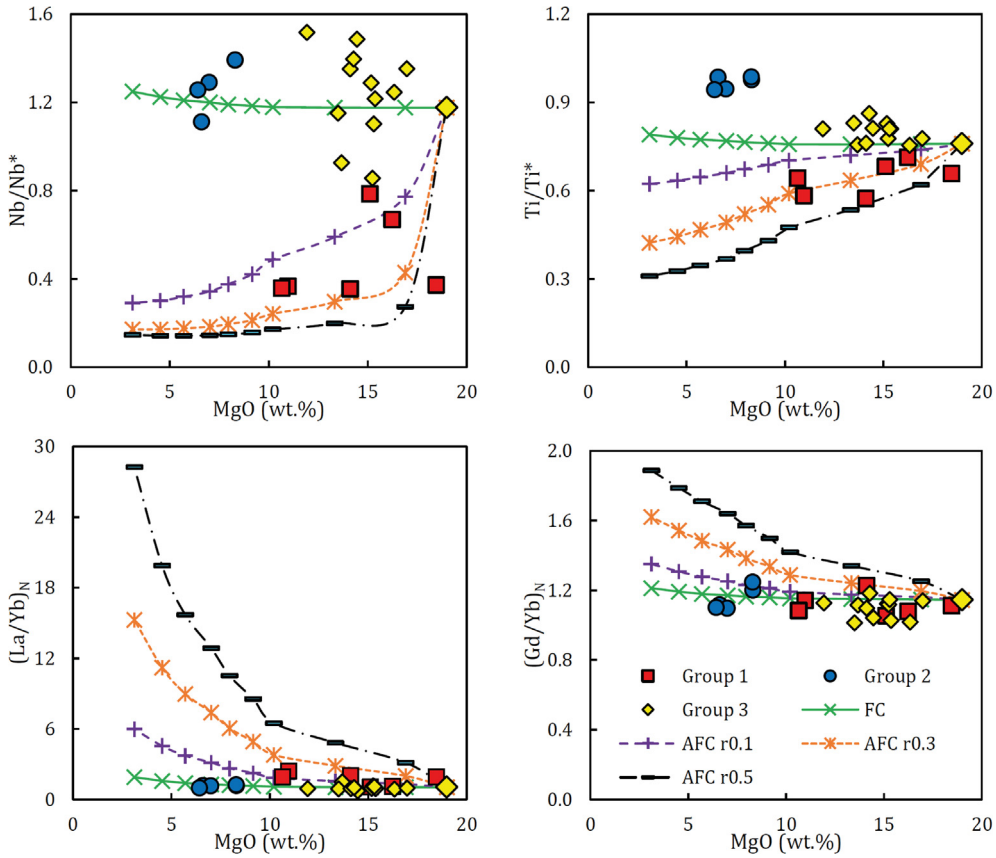

Fig. 9. Bivariate diagrams showing the trace element evolution of the Chukotat Group parental magma (MMC08-14) during fractional crystallisation under at 1 kbar pressure (anhydrous) and assimilation-fractional crystallisation (AFC) at 1 kbar pressure (anhydrous) at different r values using Felsic Continental Crust (Rudnick & Gao, 2003) as the contaminant. Markers indicate increments of 10% crystallisation. See text for description of models.

Table 6
Summary of the modelling of selected Circum-Superior LIP suites.

Suite	Parent MgO (wt%)	Pressure (kbar)	Parent H_2O (wt%)	Liquidus (°C)	Crystallisation sequence	Mechanism
Chukotat Group	18.99	1	0.5	1428	ol, cpx, sp, pl, opx	AFC (Group 1)FC (Group 2 & 3)
Flaherty Formation	7.89	1	1	1185	ol, sp, cpx, pl	FC (Group 1)AFC (Group 2)
Fox River Belt	20.59	1	0	1560	sp, ol, cpx	FC
Hellancourt Formation	9.65	1	1	1218	ol, sp, cpx, pl	FC
Hemlock Formation	8.32	1	1	1184	ol, sp, cpx, pl, opx	AFC
Kiernan Sills	10.47	1	0	1288	ol, pl, cpx, sp	FC
Molson dykes	20.45	1	0	1470	ol, sp, cpx, pl	FC
Winnipegosis Belt	25.34	1	0	1569	ol, sp, opx, pl, cpx	FC

This summary shows the MgO content of the parent magma modelled, the most successful model parameters, the predicted crystallisation sequence and the preferred mechanism for each of the Circum-Superior LIP suites studied. sp, spinel; ol, olivine; cpx, clinopyroxene; pl, plagioclase feldspar; opx, orthopyroxene. Full model results are presented in Electronic Appendix 4.

Nb-Ta and Ti anomalies) present in the CSLIP. Instead partial melts from the same mantle reservoirs have been modelled using the amount of olivine fractionation predicted by PRIMELT (Table 7) with the concomitant assimilation of upper continental crust (Rudnick and Gao, 2003). This modelling is somewhat equivocal as all modelled reservoirs can produce Nb-Ta and Ti anomalies. However partial melts from a PM-like reservoir with AFC of upper continental crust can best replicate the elemental fingerprint of the Emperor Volcanic Complex and Molson dykes (Fig. 13b).

Samples with 'Signature 3' are characterised by LREE depletions relative to the HREE, and negative Ti anomalies with no associated negative Nb-Ta anomalies making contamination with continental material an unlikely explanation. There are two potential mechanisms whereby a negative Ti anomaly might be generated in a primary magma. One is through the fractionation of phases within which Ti is compatible but Nb and Ta are not (e.g., magnetite (Nielsen et al., 1992)). However, given that the samples with this signature contain >18 wt% MgO, it is highly unlikely they have fractionated magnetite, which usually crystallises from much more evolved magmas (e.g., Ariskin et al., 1998). In a second mechanism, the primary magmas are generated from magnetite-bearing peridotite that could retain significant amounts of Ti. Primary magnetite in the mantle is difficult to distinguish from secondary magnetite that can form during serpentinisation of mantle xenoliths (Facer et al., 2009). However, recent work (Ferré et al., 2013; 2014) has shown that primary magnetite can exist in the upper mantle, albeit in amounts which vary with tectonic setting. If this magnetite had been refractory during partial melting, Ti would be retained in the residue leaving any partial melts relatively depleted. Modifying the modes of spinel lherzolite

Table 7
Primary magma compositions for different Circum-Superior LIP suites as calculated by Primelt. T – eruption temperature (°C), T_P – mantle potential temperature (°C) [† – calculated using method of Herzberg and Asimov (2015); * – calculated using method of Lee et al. (2009)], F – degree of melting, Fo – forsterite content of olivine in equilibrium with the melt,% Ol – percentage of olivine added to the sample composition in order to obtain primary magma composition.

Suite	SiO_2	TiO_2	Al_2O_3	Cr_2O_3	Fe_2O_3	FeO	MnO	MgO	CaO	Na_2O	K_2O	NiO	P_2O_5	T	$T_P^{\dagger}$	T_P^{*}	F	Fo	% Ol
Chukotat group																			
MMC08-23	49.30	0.49	9.86	0.23	1.14	9.42	0.17	17.98	9.91	1.35	0.03	0.08	0.04	1400	1512	1508	32.2	91.5	2.63
MMC08-8	49.66	0.53	8.97	0.18	1.04	9.45	0.16	18.14	10.10	1.55	0.07	0.12	0.04	1405	1516	1512	33.2	91.6	11.97
MMC08-22	48.07	0.54	9.56	0.17	1.12	9.88	0.17	19.17	9.80	1.14	0.21	0.10	0.05	1422	1542	1553	32.4	91.8	10.05
MMC08-9	50.17	0.54	9.15	0.23	1.08	9.17	0.16	17.39	10.32	1.59	0.07	0.10	0.04	1391	1497	1487	32.6	91.4	5.36
MMC08-10	48.50	0.62	9.35	0.18	1.07	9.82	0.17	19.02	9.57	1.44	0.09	0.13	0.05	1421	1538	1545	38.0	91.8	13.19
MMC08-25	49.30	0.55	9.10	0.23	1.09	9.57	0.17	18.49	9.74	1.49	0.11	0.12	0.04	1412	1525	1524	33.3	91.7	8.44
MMC08-19	47.03	0.50	8.84	0.24	1.18	10.40	0.18	20.72	9.45	1.01	0.28	0.13	0.04	1451	1581	1610	34.0	92.1	10.22
Fox river belt																			
MMFR08-10	47.39	0.48	8.74	0.32	1.25	10.50	0.19	21.60	8.87	0.45	0.05	0.13	0.04	1458	1604	1630	38.0	92.3	4.70
MMFR08-13	47.19	0.42	9.00	0.23	1.14	10.41	0.18	20.84	9.75	0.61	0.06	0.13	0.04	1446	1585	1612	28.4	92.2	14.98
Winnipegosis belt																			
MMW07-2	45.57	0.55	7.85	0.33	1.27	10.75	0.18	23.87	8.44	0.97	0.09	0.12	0.03	1505	1660	1725	28.8	93.1	7.01
MMW07-9	46.12	0.48	7.25	0.34	1.18	10.30	0.16	24.93	8.02	0.89	0.10	0.14	0.08	1519	1686	1748	36.6	93.6	11.14
MMW07-12	45.97	0.53	7.95	0.29	1.15	10.34	0.18	24.42	8.05	0.91	0.07	0.11	0.04	1510	1673	1732	34.3	93.5	15.49
Molson dykes																			
MMM07-7	45.98	0.65	9.01	0.22	1.18	10.36	0.19	22.22	8.66	1.31	0.09	0.08	0.05	1479	1619	1666	27.2	92.8	10.83
MMM07-20	47.53	0.63	9.93	0.20	1.15	10.01	0.20	19.38	9.46	1.28	0.11	0.08	0.04	1427	1548	1563	31.4	91.9	8.46
Emperor volcanic complex																			
MME08-1	48.24	0.67	12.49	0.05	0.83	8.50	0.15	15.11	10.35	1.25	2.22	0.08	0.06	1359	1438	1430	24.4	91.3	18.54

Table 8
Mantle potential temperatures and melting pressures of calculated primary magmas as calculated by FractionatePT (Lee et al., 2009). Depths calculated assuming a pressure gradient of 1 GPa/40 km.

Suite	T_P (°C)	P (GPa)	Depth (km)
Chukotat group			
MMC08-23	1508	1.96	78.36
MMC08-8	1512	1.99	79.58
MMC08-22	1553	2.56	102.50
MMC08-9	1487	1.73	68.91
MMC08-10	1545	2.46	98.31
MMC08-25	1523	2.14	85.52
MMC08-19	1610	3.38	135.00
Fox river belt			
MMFR08-10	1630	3.28	131.01
MMFR08-13	1612	3.17	126.70
Winnipegosis belt			
MMW07-2	1725	5.52	220.88
MMW07-9	1748	5.82	232.63
MMW07-10	1631	3.94	157.64
MMW07-12	1732	5.55	222.19
MMW07-18	1648	4.03	161.01
Molson dykes			
MMM07-7	1666	4.50	180.11
MMM07-20	1563	2.78	111.26
Emperor volcanic complex			
MME08-1	1430	2.00	80.14

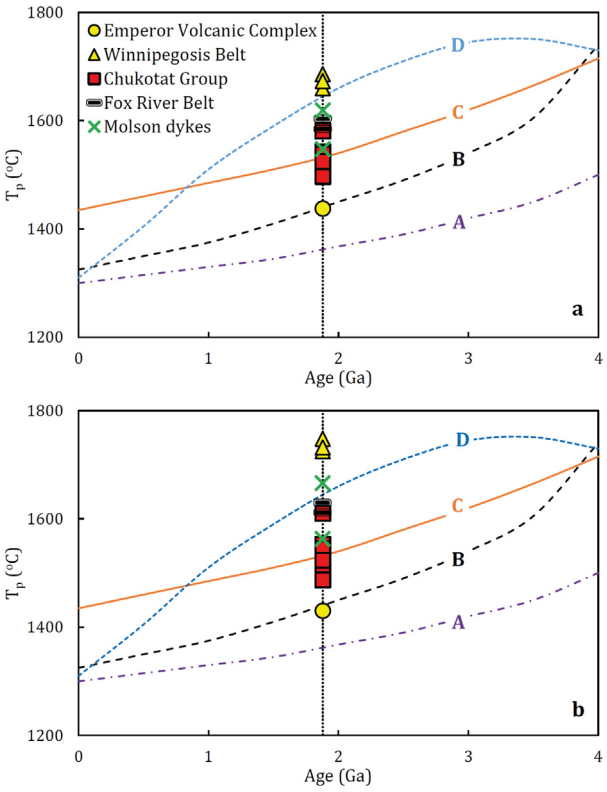

Fig. 10. Thermal evolution of the upper mantle through time using different models: A – Davies (2009); B – Richter (1988); C – Abbott et al. (1994); D – Herzberg et al. (2010). Also plotted are the T_Ps of the samples for which PRIMELT was successful in calculating a primary magma composition using the models of (a) Herzberg and Asimow (2015) and (b) Lee et al. (2009).

(Johnson et al., 1990) to include 1% magnetite can produce magmas which fractionate to produce mafic melts with pronounced negative Ti anomalies (Fig. 13c). However, without defined phase proportions (including magnetite) in both the reservoir and melt fractions, any modelling is speculative.

Samples with 'Signature 4' are characterised by relatively flat REE trends, positive Nb-Ta anomalies and $(Th/Nb)_N < 1$. These characteristics are often attributed to the inclusion of significant amounts of recycled oceanic crust in the source region (e.g., Hofmann, 1997). In an attempt to investigate this, each of the three mantle reservoirs had 10% subducted ocean crust (SOC) added to them (SOC = 25% NMORB (Hofmann, 1988), 25% altered MORB (Staudigel et al., 1996), and 50% average gabbro 735B (Hart et al., 1999)). Prior to its inclusion in each of the mantle reservoirs, the trace element composition of the SOC was modified to take into account sub-arc alteration processes using the mobility modifiers of Kogiso et al. (1997) and Stracke (2003). The 30% partial melts produced by these modified reservoirs were then fractionated to remove 12% olivine (predicted by PRIMELT for Chukotat Group sample MMC08-10 and Molson dyke sample MMM07-7). This

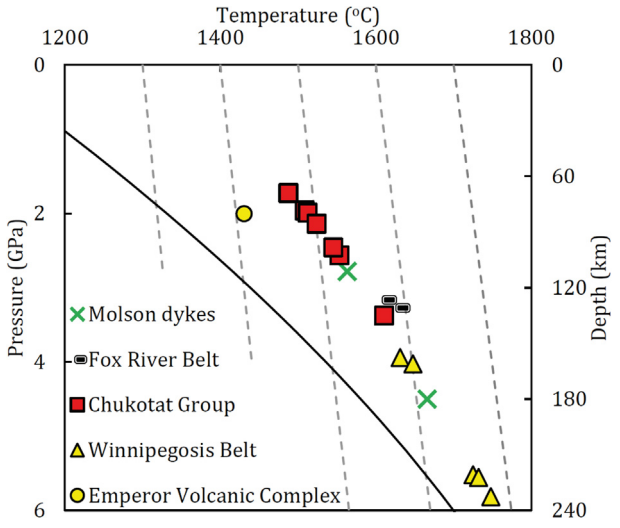

Fig. 11. Temperatures and pressures calculated for primary magmas of Circum-Superior LIP suites as calculated by FractionatePT (Lee et al., 2009). Peridotite solidus from Hirschmann et al. (2003). Dashed lines correspond to isentropic melting adiabats.

modelling (Fig. 13d) shows that no single reservoir is capable of replicating the composition of 'Signature 4', but that individual reservoirs are capable of modelling certain aspects. For example, partial melts from the modified EM1 and DMM reservoirs are capable of replicating the magnitude of the $(Th/Nb)_N < 1$, while the modified DMM reservoir alone can reproduce the magnitude of the Nb-Ta anomalies. Finally, though all modified reservoirs modelled produce magmas with flat HREE abundances, all of the magmas modelled record much greater HREE abundances than the samples studied. This may suggest that the source regions for some sections of the CSLIP are more depleted than those modelled, potentially via re-melting of material that was already depleted during the production of the 1.90 – 1.99 Ga Povungnituk, Mugford, Minto Eskimo and Hearne-Chipman-Snowbird LIPs, all of which are spatially associated with the margins of the Superior Province (Ernst and Bleeker, 2010).

In summary, the primary magmas of the Circum-Superior LIP have been derived from a number of different mantle sources. These were similar in composition to the modern mantle reservoirs of EM1, DMM, and PM, some of which may have contained primary magnetite, and others which appear to have included significant amounts of recycled oceanic crust. Nd and Hf isotope data reveal that the samples analysed in this study have Nd-Hf ranging from depleted to slightly enriched (Fig 12). Therefore, following extraction from the mantle, some of the primary magmas were likely contaminated by crustal material during crystal fractionation as previously argued from trace element considerations.

4.6. Distribution of CSLIP magmatism

The majority of CSLIP magmatic rocks are preserved along the cratonic margins of the Superior Province. This distribution has been used as an argument against a mantle plume origin for the LIP (French et al., 2008; Heaman et al., 2009). In this section we will review possible explanations for the largely peripheral distribution of CLIP suites around the craton. The model must also account for the Pickle Crow and Fort Albany dykes in the interior of the craton and the carbonatites along the Kapuskasing Structural Zone (Ernst and Bell, 2010).

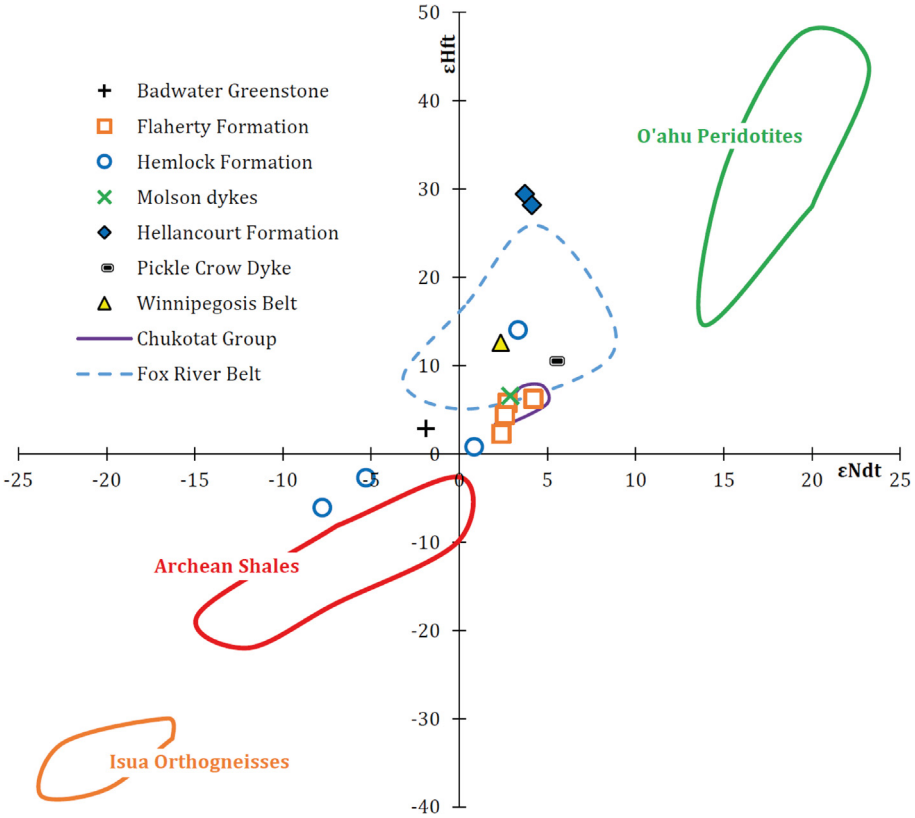

Fig. 12. Variation of εNdt vs εHft for the Circum-Superior LIP suites analysed in this study (t = 1880 Ma). For comparison, fields for other Archean–Paleoproterozoic components are plotted: Isua Orthogneisses and Archean Shales; O'ahu peridotite mantle xenoliths (Bizimis et al., 2007). Fields for Chukotat Group and Fox River Belt rocks are from Blichert-Toft and Arndt (1999), Vervoort and Blichert-Toft (1999) and Desharnais (2005).

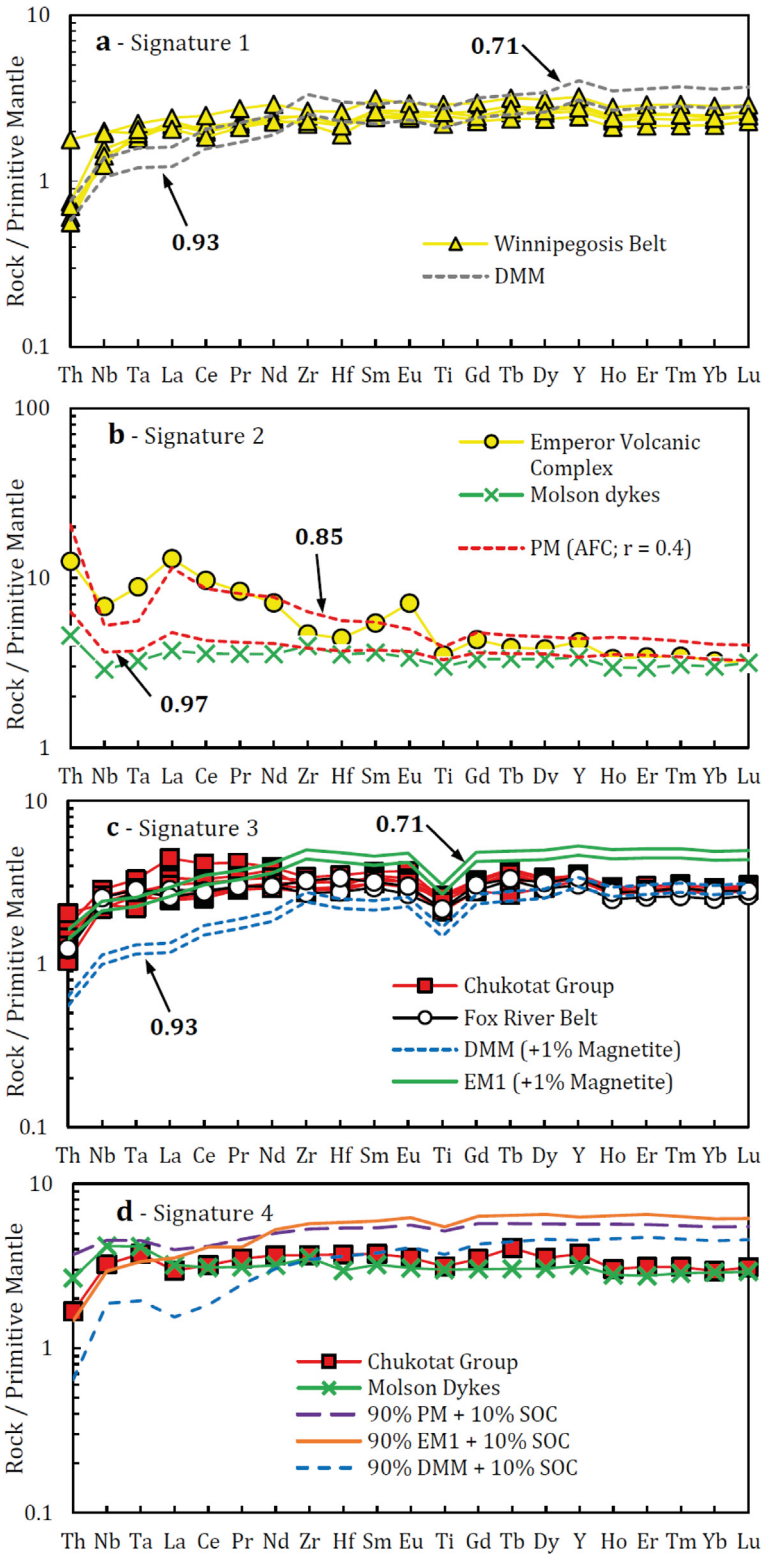

Fig. 13. Primitive mantle normalised trace element diagrams showing the four trace element 'signatures' present in the Circum-Superior LIP as recorded by samples for which PRIMELT calculated primary magmas. Reservoir lines (without markers) show 30% partial melts from selected mantle reservoirs which have had olivine fractionated to the degree specified. In b, fractionation was modelled with concomitant assimilation of upper continental crust (Rudnick & Goa, 2003) and a 30% partial of Primitive mantle at an assimilation/fractionation ratio of 0.4. In (d), melting of mantle reservoirs which have been modified to include 10% of subducted ocean crust (SOC) and 12% subsequent fractionation. Normalising factors taken from McDonough and Sun (1995).

4.6.1. Plume head flattening

Plume heads are predicted to have a diameter of ~2000–2500 km once the plume flattens beneath the lithosphere (Campbell, 2007). A plume head with these dimensions is approximately the same size as the Superior Province and if the plume centre point impinged beneath the centre of the craton then the margins of the plume could have melted to form the CSLIP. However, a lack of ~1880 Ma magmatic rocks located on the

southeastern margin of the Superior Province appears not to support this model. Furthermore, the Molson dykes, Pickle Crow dyke and Fort Albany dykes possibly form a radiating dyke swarm which converge to a focal point just to the north of the northwest Superior Province margin, suggesting that the plume impinged beneath this part of the craton rather than the centre (Buchan et al., 2003; Hamilton and Stott, 2008; Ernst and Bleeker, 2010; Ernst and Bell, 2010).

4.6.2. Magma transportation via dykes

Radiating dyke swarms are commonly linked to mantle plumes and are often used to locate the centre of the plume head (e.g., Ernst et al., 1995; Ernst and Buchan, 2003; Ernst, 2014). Radiating dyke swarms can transport magma huge distances from the plume centre, the longest known on Earth being the ~1270 Ma Mackenzie dyke swarm which extends ~2500 km southeastwards through the Canadian Shield (Ernst and Baragar, 1992; Baragar et al., 1996). Thus, the transportation of magma from the plume centre through large dykes such as the ~600 km long Pickle Crow dyke may account for the magmatism which occurred in the Lake Superior region (e.g., Minifie et al., 2013). However, the Cape Smith Belt and Labrador Trough are not spatially associated with any known radiating dykes of ~1880 Ma age (e.g., Maurice and Francis, 2010) although many dyke sets in northern Quebec remain to be dated. Also the eastern and western halves of the Superior craton opened about 23 degrees with movement along the Kapuskasing Structural Zone (Evans and Halls, 2010). The timing of this opening is post-2070 Ma, but has unknown timing with respect to the 1880 Ma event. If this rotational opening postdated the Circum-Superior 1880–1870 Ma LIP, then the 1880 Ma magmatism in the Cape Smith belt and Labrador Trough would originally have been about 500 km closer to the Thompson centre (at the focus of the radiating swarm).

4.6.3. Deflection of plume material to regions of thinner lithosphere

Seismic studies suggest that the thickness of the cratonic root of the Superior Province may be ~300 km (van der Lee and Nolet, 1997). The major element chemistry of the primary magmas from the Chukotat Group, Fox River Belt, Winnipegosis Belt and Molson dykes indicates that melting in these regions occurred at pressures corresponding to a range in the depth of melting of ~115–180 km. Large scale melting is therefore unlikely to have occurred under the thickest lithosphere of the Superior Province.

Sleep et al. (2002) have modelled the effects of cratonic keels on plume magmatism and shown that keels will deflect plume material and result in flow up steep gradients along the base of the lithosphere and focus melting along the cratonic boundaries. Models such as this find support in work of Thompson and Gibson (1991) and Johnston and Thorkelson (2000) who proposed that, in regions of differing lithosphere thickness, plume material will migrate to thinspots where large amounts of decompression melting can occur.

Evidence of lithospheric thinning around the margins of the Superior province can be observed in close proximity to some of the CSLIP magmatism. This is particularly evident in the Cape Smith Belt, where the 2.04–1.96 Ga magmatism of the Povungnituk Group is proposed to have formed during rifting of the Superior Province margin (e.g., Parrish, 1989; Ernst and Bleeker, 2010). This rifting would have led to thinning of the lithosphere directly beneath the Cape Smith Belt prior to the ~1880 Ma Circum-Superior magmatic event.

In the case of the Labrador Trough magmatism, the ~1.88 Ga CSLIP magmatism is preceded by an older (~2.17–2.15 Ga) cycle of magmatism that may also reflect rifting and thinning of the lithosphere beneath the northeastern margin of the Superior Province ~275 m.y. prior to the CSLIP magmatism (Rohon et al., 1993; Ernst and Bleeker, 2010). There is also evidence of rifting ~200 m.y. prior to the emplacement of the Thompson Nickel Belt near the northwest Superior Province margin in the form of the 2091 ± 2 Ma Cauchon dykes (Halls and Heaman, 2000). The southwestern margin of the Superior Province also appears to have been affected by significant magmatic activity at ~2.1 Ga including the Marathon, Kapuskasing and Fort Frances dyke swarms (Marathon LIP; Halls et al., 2008).

The deflection of plume material away from the cratonic keel towards regions of thinner lithosphere at the cratonic margins is an attractive theory for the CSLIP. It is consistent with the observation that the cratonic margins where ~1880 Ma magmatic rocks are found are located in regions affected by large magmatic and rifting events < 300 m.y. before which may have thinned the lithosphere under these margins. This can also explain why there are no ~1880 Ma magmatic rocks along the southeastern margin of the Superior Province since the largest magmatic events prior to the CSLIP which affected the southeastern margin of the Superior Province are over 300 m.y. older than the CSLIP (e.g., Halls et al., 2005; Ketchum et al., 2013). This time-span was likely to have been long enough to allow the lithosphere beneath the southeast Superior Province margin to thicken sufficiently such that plume material did not flow along the base of this lithosphere at 1.88 Ga. The deflection of plume material by a thick cratonic keel towards thinner lithosphere at a rifted craton margin has also been proposed for ~2.7 Ga magmatism in the Yilgarn craton of Western Australia (e.g., Said et al., 2010).

4.6.4. Non-plume-related edge-driven convection

An alternative explanation to the mantle plume hypothesis for the occurrence of LIPs close to the edges of Archaean cratons was advocated by King and Anderson (1995) who suggest that the thick cratonic lithosphere insulates the underlying asthenospheric mantle which then flows out sideways from under the craton, upwells, decompresses and melts under thinner continental lithosphere. This model does not require mantle temperatures as hot as for the plume model.

The edge-driven convection model may be more appropriate for some magmatic provinces than the mantle plume model (King, 2007) but it does not seem applicable to the CSLIP. As noted by Saunders et al. (2005), the edge-driven convection model has no obvious trigger or switch-off mechanism and could potentially last for several tens of millions of years, unlike the ~15 m.y. for the majority of ultramafic-mafic magmatism of the CSLIP (Fig. 2). The presence of magmatic rocks (i.e., mafic dykes and carbonatite complexes) in the interior of the Superior Province craton is also inconsistent with the edge-driven convection model which has no mechanism for generating magmatism away from the craton margins. It is also hard to envisage how the high MgO picrites of the CSLIP can be produced without the high mantle potential temperatures of a plume.

5. Conclusions

1. The CSLIP is an unusual LIP in that the majority of it is distributed along >3000 km of the margins of the Superior Province.
2. The earliest preserved magmatic activity of the CSLIP may be represented by carbonatitic magmatism along the Kapuskasing Structural Zone which has an age range of 1897–1907 Ma. Most of the ultramafic-mafic magmatism of the LIP occurred between 1885 Ma and 1870 Ma (Fig. 2). The final manifestation of Circum-Superior magmatism comprises picrites and basalts of the Winnipegosis Belt (1864 Ma).

3. A common geodynamic origin for the various segments of the CSLIP is supported by similar incompatible trace element signatures in most of the magmatic segments. This trace element signature is similar to that of modern oceanic plateaus such as the Ontong Java Plateau and can be derived from a mantle source composition intermediate between the modern day DMM and EM1 mantle reservoirs. Uncontaminated CSLIP samples have positive εNdi values also suggesting derivation from a depleted mantle source.
4. Much of the trace element variation between the different segments and within individual segments can be accounted for by differing degrees of partial melting, fractional crystallisation or crustal contamination. In Hf-Nd isotopic space, some of the CSLIP samples appear to define mixing trends between a depleted mantle end member and estimates of the Proterozoic continental crust.
5. Modelling shows that the CSLIP formed from mantle with a T_p up to 274 °C hotter than some of the estimates for the ambient upper mantle at ~1880 Ma. Major element modelling also shows that partial melting, at least beneath the Cape Smith Belt and the Thompson Salient, occurred relatively deep at pressures ranging from 3.8 to 6 GPa (~115–180 km). The lack of a residual mantle garnet signature in the trace element patterns of these rocks is most likely because the degree of partial melting was high enough to consume all of the garnet in the source region.
6. Although most previous studies on the CSLIP have advocated the generation of this igneous province from a shallow depleted upper mantle, the conclusion of this study is that the CSLIP was formed by melting of a deep mantle plume. This plume impinged beneath the Superior Province craton where it was deflected towards regions of thinner lithosphere at the previously-rifted cratonic margins. Evidence for a mantle plume origin includes the high MgO and Ni content of many rocks, the oceanic-plateau-like incompatible trace element profiles, the possible presence of a small OIB component, the calculated high degrees of partial melting, and the high mantle T_p. One major concentration is on the NW side of the Superior craton where a radiating swarm is present.

Acknowledgements

MJM acknowledges NERC PhD studentship NER/S/A/2006/14009 and funding by BHP Billiton. REE was partially supported by the Russian Government (grant No. 14.Y26.31.0012). Iain McDonald, Anthony Oldroyd, and Ley Woolley are thanked for their laboratory assistance. Gerry Benger, Ken Buchan, Tim Corkery, Guy Desharnais, Don Francis, Norman Halden, Henry Halls, Larry Hulbert, Steve Kissin, Dan Layton-Matthews and James Mungall are thanked for their invaluable help in providing rock samples for this work, either by generously allowing access to their own sample collection or by kindly assisting in the search for suitable rock samples. Steve Kissin also kindly helped in the field collection around the Lake Superior region. Sarah Albone is thanked for insightful discussions regarding chemistry.

Appendix A. Supplementary data

Supplementary data associated with this article can be found, in the online version, at http://dx.doi.org/10.1016/j.precamres.2017.03.001.

References

Anderson, D.L., 1982. Hotspots, polar wander, Mesozoic convection and the geoid. Nature 297, 391–393.
Anderson, D.L., 2000. The thermal state of the upper mantle; no role for mantle plumes. Geophys. Res. Lett. 27, 3623–3636.
Ariskin, A.A. et al., 1998. Simulating low-pressure tholeiite-magma fractional crystallization. Geochem. Int. 25 (4), 21–37.
Arndt, N.T., 2003. Komatiites, kimberlites, and boninites. J. Geophys. Res. 108. http://dx.doi.org/10.1029/2002JB002157.
Baragar, W.R.A. 2007. Geology, Ottawa Islands, eastern Hudson Bay, Nunavut. Geological Survey of Canada, Map 2113A.
Baragar, W.R.A. 2007. Geology, Sleeper Islands, eastern Hudson Bay, Nunavut. Geological Survey of Canada, Map 2114A.
Baragar, W.R.A. 2008. Geology, Smith Island and adjoining mainland, eastern Hudson Bay, Nunavut-Quebec. Geological Survey of Canada, Map 2112A.
Baragar, W.R.A., Lamontagne, C.G., 1980. The Circum-Ungava Belt in eastern Hudson Bay; the geology of Sleeper Islands and parts of the Ottawa and Belcher Islands. Current Research Part A. Geological Survey of Canada Paper 80-1A. Geological Survey of Canada, Ottawa, pp. 89–94.
Baragar, W.R.A., Scoates, R.F.J., 1981. The Circum-Superior Belt; a Proterozoic plate margin? In: Kroener, A. (Ed.), Precambrian Plate Tectonics. Elsevier, Amsterdam, pp. 297–330.
Baragar, W.R.A., Scoates, R.F.J., 1987. Volcanic geochemistry of the northern segments of the Circum-Superior Belt of the Canadian Shield. In: Pharaoh, T. C., Beckinsale, R.D., Rickard, D. (Eds.), Geochemistry and mineralization of Proterozoic volcanic suites, Geological Society Special Publication, vol. 33. Geological Society of London, London, pp. 113–145.
Baragar, W.R.A., Ernst, R.E., Hulbert, L.J., Peterson, T., 1996. Longitudinal petrochemical variation in the Mackenzie dyke swarm, northwestern Canadian Shield. J. Petrol. 37, 317–359.
Bédard, J.H., 2001. Parental magmas of the Nain Plutonic Suite anorthosites and mafic cumulates: a trace element modelling approach. Contrib. Miner. Petrol. 141 (6), 747–771.
Bell, K., Blenkinsop, J., Kwon, S.T., Tilton, G.R., Sage, R.P., 1987. Age and radiogenic isotopic systematics of the Borden carbonatite complex, Ontario, Canada. Can. J. Earth Sci. 24, 24–30.
Bizimis, M., Griselin, M., Lassiter, J.C., Salters, V.J.M., Sen, G., 2007. Ancient recycled mantle lithosphere in the Hawaiian plume: osmium-hafnium isotopic evidence from peridotite mantle xenoliths. Earth Planet. Sci. Lett. 257, 259–273.
Bleeker, Ernst, R.E., 2006. Short-lived mantle generated magmatic events and their dyke swarms: the key to unlocking Earth's paleogeographic record back to 2.6 Ga. In: Hanski, E., Mertanen, S., Ramo, T., Vuollo, J. (Eds.), Dyke Swarms – Time Markers of Crustal Evolution. Taylor & Francis, London, pp. 3–26.
Blichert-Toft, J., Arndt, N.T., 1999. Hf isotope compositions of komatiites. Earth Planet. Sci. Lett. 171, 439–451.
Bostock, H.H., 1971. Geological notes on Aquatuk River map-area, Ontario, with emphasis on the Precambrian rocks. Geological Survey of Canada Paper 70–42. Geological Survey of Canada, Ottawa. 57pp.
Bryan, S., Ernst, R.E., 2008. Revised definition of Large Igneous Provinces (LIPs). Earth-Sci. Rev. 86, 175–202.
Bryan, S.E., Ferrari, L., 2013. Large igneous provinces and silicic large igneous provinces: Progress in our understanding over the last 25 years. Geol. Soc. Am. Bull. 125, 1053–1078.
Buchan, K.L., Harris, B.A., Ernst, R.E., Hanes, J.A., 2003. Ar-Ar dating of the Pickle Crow diabase dyke in the western Superior craton of the Canadian Shield of Ontario and implications for a possible plume centre associated with ca. 1880 Ma Molson magmatism of Manitoba. Geological Association of Canada-Mineralogical Association of Canada Annual Meeting 2003. Program with Abstracts 28, pp. 17.
Buchan, K.L., Mortensen, J.K., Card, K.D., Percival, J.A., 1998. Paleomagnetism and U-Pb geochronology of diabase dyke swarms of Minto block, Superior Province, Quebec, Canada. Can. J. Earth Sci. 35, 1054–1069.
Burnham, O.M., Halden, N.M., Layton-Matthews, D., Lesher, C.M., Liwanag, J., Heaman, L.M., Hulbert, L.J., Machado, N., Michalak, D., Pacey, M., Peck, D.C., Potrel, A., Theyer, P., Toope, K., Zwanzig, H.V. 2004. Geology, stratigraphy, petrogenesis, and metallogenesis of the Thompson Nickel Belt, Manitoba: final report for CAMIRO Project 97E-02. Mineral Exploration Research Centre, Laurentian University, Sudbury. 410pp.
Campbell, I.H., 2007. Testing the plume theory. Chem. Geol. 241, 153–176.
Cann, J.R., 1970. Rb, Sr, Y, Zr and Nb in some ocean floor basaltic rocks. Earth Planet. Sci. Lett. 10, 7–11.
Cao, Q., van der Hilst, R.D., de Hoop, M.V., Shim, S.-H., 2011. Seismic imaging of transition zone discontinuities suggests hot mantle west of Hawaii. Science 332, 1068–1071.
Card, K.D., Ciesielski, A., 1986. DNAG No. 1. Subdivisions of the Superior Province of the Canadian Shield. Geosci. Can. 13, 5–13.
Chauvel, C., Hofmann, A.W., Vidal, P., 1992. HIMU-EM: the french polynesian connection. Earth Planet. Sci. Lett. 110, 99–119.
Cheve, S.R., Machado, N. 1988. Reinvestigation of the Castignon Lake carbonatite complex, Labrador Trough, New Quebec. Geological Association of Canada-Mineralogical Association of Canada Annual Meeting 1988. Program with Abstracts 13, pp. 20.
Ciborowski, T.J.R., Kerr, A.C., 2016. Did mantle plume magmatism help trigger the Great Oxidation Event? Lithos 246–247, 128–133.
Ciborowski, T.J.R. et al., 2015. The early proterozoic matachewan large igneous province: geochemistry, petrogenesis, and implications for earth evolution. J. Petrol. 56 (8), 1459–1494.

Coffin, M.F., Eldholm, O., 1994. Large igneous provinces: crustal structure, dimensions, and external consequences. Rev. Geophys. 32, 1–36.
Coffin, M.F., Eldholm, O., 2005. Large igneous provinces. In: Selley, R.C., Cocks, R., Plimer, I.R. (Eds.), Encyclopedia of Geology, pp. 315–323.
Coltice, N., Bertrand, H., Rey, P., Jourdan, F., Phillips, B.R., Ricard, Y., 2009. Global warming of the mantle beneath continents back to the Archaean. Gondwana Res. 15, 254–266.
Condie, K.C., 2005. High field strength element ratios in Archean basalts: a window to evolving sources of mantle plumes? Lithos 79, 491–504.
Craddock, J.P., Anziano, J., Wirth, K., Vervoort, J.D., Singer, B., Zhang, X., 2007. Structure, geochemistry and geochronology of a Penokean lamprophyre dike swarm, Archean Wawa Terrane, Little Presque Isle, Michigan, USA. Precambr. Res. 157, 50–70.
Davies, G.F., 2009. Effect of plate bending on the Urey ratio and the thermal evolution of the mantle. Earth Planet. Sci. Lett. 287, 513–518.
Desharnais, G., 2005. Geochemical and Isotopic Investigation of Magmatism in the Fox River Belt: Tectonic and Economic Implications PhD thesis. University of Manitoba, Winnipeg. 207pp.
Dimroth, E., Baragar, W.R.A., Bergeron, R., Jackson, G.D., 1970. The filling of the Circum-Ungava geosyncline. In: Baer, A.J. (Ed.), Basins and geosynclines of the Canadian Shield. Geological Survey of Canada Paper 70-40. Geological Survey of Canada, Ottawa, pp. 45–142.
Elkins-Tanton, L.T., 2007. Continental magmatism, volatile recycling, and a heterogeneous mantle caused by lithospheric gravitational instabilities. J. Geophys. Res. 112, B03405.
Ernst, R.E., 2014. Large Igneous Provinces. Cambridge University Press, p. 666.
Ernst, R.E., Buchan, K.L. 2001. Large mafic magmatic events through time and links to mantle-plume heads. In: Ernst, R.E., & Buchan, K.L. (Eds.), Mantle Plumes: Their Identification Through Time, Geological Society of America Special Paper 352, Geological Society of America, Boulder. pp. 483–575.
Ernst, R.E., Baragar, W.R.A., 1992. Evidence from magnetic fabric for the flow pattern of magma in the Mackenzie giant radiating dyke swarm. Nature 356, 511–513.
Ernst, R.E., Bell, K., 2010. Large Igneous Provinces (LIPs) and Carbonatites. Mineral. Petrol. 98, 55–76.
Ernst, R.E., Buchan, K.L., 2003. Recognizing mantle plumes in the geological record. Annu. Rev. Earth Planet. Sci. 31, 469–523.
Ernst, R.E., Buchan, K.L., 2004. Igneous rock association in Canada 3. Large Igneous Provinces (LIPs) in Canada and adjacent regions: 3 Ga to present. Geosci. Can. 31, 103–126.
Ernst, R.E., Head, J.W., Parfitt, E., Grosfils, E., Wilson, L., 1995. Giant radiating dyke swarms on Earth and Venus. Earth-Sci. Rev. 39, 1–58.
Ernst, R.E., Buchan, K.L., Campbell, I.H., 2005. Frontiers in large igneous province research. Lithos 79, 271–297.
Evans, D.A.D., Halls, H.C., 2010. Restoring Proterozoic deformation within the Superior craton. Precambr. Res. 183, 474–489.
Facer, J., Downes, H., Beard, A., 2009. In situ Serpentinization and Hydrous Fluid Metasomatism in Spinel Dunite Xenoliths from the Bearpaw Mountains, Montana, USA 50, 1443–1475.
Ferré, E.C. et al., 2013. The magnetism of mantle xenoliths and potential implications for sub-Moho magnetic sources. Geophys. Res. Lett. 40 (1), 105–110.
Ferré, E.C. et al., 2014. Eight good reasons why the uppermost mantle could be magnetic. Tectonophysics 624–625, 3–14.
Findlay, J.M., Parrish, R.R., Birkett, T.C., Watanabe, D.H., 1995. U-Pb ages from the Nimish Formation and Montagnais glomeroporphyritic gabbro of the central New Quebec Orogen, Canada. Can. J. Earth Sci. 32, 1208–1220.
Fitton, J.G., Godard, M., 2004. Origin and evolution of magmas on the Ontong Java Plateau. In: Origin and evolution of the Ontong Java Plateau. In: Fitton, J.G., Mahoney, J.J., Wallace, P.J., Saunders, A.D. (Eds.), . Geological Society Special Publication, vol. 229. Geological Society of London, London, pp. 151–178.
Fralick, P.W., Davis, D.W., Kissin, S.A., 2002. The age of the Gunflint Formation, Ontario, Canada: single U-Pb age determinations from reworked volcanic ash. Can. J. Earth Sci. 39, 1085–1091.
French, J.E., Heaman, L.M., Chacko, T., Srivastava, R.K., 2008. 1891–1883 Ma Southern Bastar-Cuddapah mafic igneous events, India: a newly recognized large igneous province. Precambr. Res. 160, 308–322.
Gair, J.E., Wier, K.L., 1956. Geology of the Kiernan quadrangle, Iron County, Michigan. US Geological Survey Bulletin 1044. US Government Printing Office, Washington DC. 88pp.
Galer, S.J.G., Mezger, K., 1998. Metamorphism, denudation and sea level in the Archean and cooling of the Earth. Precambr. Res. 92, 389–412.
Gibb, R.A., Walcott, R.I., 1971. A Precambrian suture in the Canadian Shield. Earth Planet. Sci. Lett. 10, 417–422.
Gualda, G.A.R., Ghiorso, M.S., 2015. MELTS_Excel: AMicrosoft Excel-based MELTS interface for research and teaching of magma properties and evolution. Geochem. Geophys. Geosyst. 16 (1), 315–324.
Halls, H.C., Heaman, L.M., 2000. The paleomagnetic significance of new U-Pb age data from the Molson dyke swarm, Cauchon Lake area, Manitoba. Can. J. Earth Sci. 37, 957–966.
Halls, H.C., Stott, G.M., Davis, D.W., 2005. Paleomagnetism, geochronology and geochemistry of several Proterozoic mafic dike swarms in northwestern Ontario. Ontario Geol. Survey, 59. Open File Report 6171.
Halls, H.C., Davis, D.W., Stott, G.M., Ernst, R.E., Hamilton, M.A., 2008. The Paleoproterozoic Marathon Large Igneous Province: new evidence for a 2.1 Ga long-lived mantle plume event along the southern margin of the North American Superior Province. Precambr. Res. 162, 327–353.
Hamilton, M.A., Stott, G.M., 2008. Project Unit 04-018. The significance of new U/Pb baddeleyite ages from two Paleoproterozoic diabase dikes in northern Ontario. In: Summary of Fieldwork and Other Activities 2008. Ontario Geological Survey Open File Report 6226. Ministry of Northern Development and Mines, Toronto. pp. 17-1–17-7.
Hamilton, M.A., Buchan, K.L., Ernst. R.E., Stott, G.M., 2009. Widespread and short-lived 1870 Ma mafic magmatism along the northern Superior craton margin. 2009 Joint Assembly (AGU, CGU, GS, GAC, IAH–CNC, MAC, MSA, SEG), 24–27 May 2009, Toronto, Ont., Canada [Abstract].
Hart, S.R. et al., 1999. The fingerprint of seawater circulation in a 500-meter section of ocean crust gabbros. Geochim. Cosmochim. Acta 63 (23–24), 4059–4080.
Hastie, A.R. et al., 2009. Geochemistry and tectonomagmatic significance of Lower Cretaceous island arc lavas from the Devils Racecourse Formation, eastern Jamaica. Geol. Soc. London, Special Publ. 328 (1), 339–360.
Heaman, L.M., Machado, N., Krogh, T.E., Weber, W., 1986. Precise U-Pb zircon ages for the Molson dyke swarm and the Fox River sill: constraints for early Proterozoic crustal evolution in northeastern Manitoba, Canada. Contrib. Miner. Petrol. 94, 82–89.
Heaman, L.M., Peck, D.C., Toope, K., 2009. Timing and geochemistry of 1.88 Ga Molson Igneous Events, Manitoba: insights into the formation of a craton-scale magmatic and metallogenic province. Precambr. Res. 172, 143–162.
Herzberg, C., 1995. Generation of plume magmas through time: an experimental perspective. Chem. Geol. 126, 1–16.
Herzberg, C., Asimow, P.D., 2015. PRIMELT3 MEGA.XLSM software for primary magma calculation: Peridotite primary magma MgO contents from the liquidus to the solidus. Geochem. Geophys. Geosyst. 16 (2), 563–578.
Herzberg, C., O'Hara, M.J., 2002. Plume-associated ultramafic magmas of Phanerozoic age. J. Petrol. 43, 1857–1883.
Herzberg, C., Zhang, J., 1996. Melting experiments on anhydrous peridotite KLB-1: compositions of magmas in the upper mantle and transition zone. J. Geophys. Res. 101, 8271–8295.
Herzberg, C., Condie, K.C., Korenaga, J., 2010. Thermal history of the Earth and its petrological expression. Earth Planet. Sci. Lett. 292, 79–88.
Hoffman, P.F., 1988. United plates of America, the birth of a craton: early Proterozoic assembly and growth of Laurentia. Annu. Rev. Earth Planet. Sci. 16, 543–603.
Hofmann, A.W., 1997. Mantle geochemistry: the message from oceanic volcanism. Nature 385, 218–229.
Hulbert, L.J., Kyser, K., Carlson, R., Lesher, C.M., Joudrie, C., 1994. The Winnipegosis Komatiites; a New Komatiite Belt, Central Manitoba. Minerals Colloquium Program with Abstracts. Geological Survey of Canada, Ottawa.
Hulbert, L.J., Hamilton, M.A., Horan, M.F., Scoates, R.F.J., 2005. U-Pb zircon and Re-Os isotope geochronology of mineralized ultramafic intrusions and associated nickel ores of the Thompson Nickel Belt, Manitoba, Canada. Econ. Geol. 100, 29–41.
Huppert, H.E., Sparks, R.S.J., 1985. Komatiites I: eruption and flow. J. Petrol. 26, 694–725.
Ingle, S., Coffin, M.F., 2004. Impact origin for the greater Ontong Java Plateau? Earth Planet. Sci. Lett. 218, 123–134.
Johnson, K.T.M., Dick, H.J.B., Shimizu, N., 1990. Melting in the oceanic upper mantle: an ion microprobe study of diopsides in abyssal peridotites. J. Geophys. Res. 95, 2661–2678.
Johnston, S.T., Thorkelson, D.J., 2000. Continental flood basalts: episodic magmatism above long- lived hotspots. Earth Planet. Sci. Lett. 175, 247–256.
Jones, A.P., 2005. Meteorite impacts as triggers to Large Igneous Provinces. Elements 1, 277–281.
Karato, S., 2010. Rheology of the Earth's mantle: a historical review. Gondwana Res. 18, 17–45.
Kerr, A.C., 2014. 4.18 – Oceanic Plateaus A2 - Holland, Heinrich D. Treatise on Geochemistry (Second Edition). K.K. Turekian. Elsevier, Oxford, pp. 631–667.
Kerr, A.C., Arndt, N.T., 2001. A note on the IUGS reclassification of the high-Mg and picritic volcanic rocks. J. Petrol. 42, 2169–2171.
Kerr, A.C., Kempton, P.D., Thompson, R.N., 1995. Crustal assimilation during turbulent magma ascent (ATA); new isotopic evidence from the Mull Tertiary lava succession, NW Scotland. Contrib. Miner. Petrol. 119, 142–154.
Ketchum, K.Y., Heaman, L.M., Bennet, G., Hughes, D.J., 2013. Age, petrogenesis and tectonic setting of the Thessalon volcanic rocks, Huronian Supergroup, Canada. Precambr. Res. 233, 144–172.
King, S.D., 2007. Hotspots and edge-driven convection. Geology 35, 223–226.
King, S.D., Anderson, D.L., 1995. An alternative mechanism of flood basalt formation. Earth Planet. Sci. Lett. 136, 269–279.
Kogiso, T.Y., Tatsumi, Y., Shimoda, G., Barsczus, H., 1997. High μ (HIMU) ocean island basalts in southern Polynesia: new evidence for whole mantle scale recycling of subducted oceanic crust. J. Geophys. Res. 102, 8085–8103.
Komiya, T., Maruyama, S., Hirata, T., Yurimoto, H., Nohda, S., 2004. Geochemistry of the oldest MORB and OIB in the Isua supracrustal belt, southern west Greenland: implications for the composition and temperature of early Archean upper mantle. Island Arch. 13, 47–72.
Korenaga, J., 2008. Urey ratio and the structure and evolution of Earth's mantle. Rev. Geophys. 46. http://dx.doi.org/10.1029/2007RG000241.
Layton-Matthews, D., Lesher, C.M., Burnham, O.M., Liwanag, J., Halden, N.M., Hulbert, L.J., Peck, D.C., 2007. Magmatic Ni-Cu-platinum-group element deposits of the Thompson Nickel Belt. In: Goodfellow, W.D. (ed) Mineral deposits of Canada: a synthesis of major deposit-types, district metallogeny, the evolution of geological provinces, and exploration models. Geological Association of Canada, Mineral Deposits Division, Special Publication No. 5.

Geological Association of Canada- Mineral Deposits Division, St. John's. pp. 409–432.
Lee, C.-T.A. et al., 2009. Constraints on the depths and temperatures of basaltic magma generation on Earth and other terrestrial planets using new thermobarometers for mafic magmas. Earth Planet. Sci. Lett. 279 (1–2), 20–33.
Lesher, C., 2007. Ni-Cu-(PGE) deposits in the Raglan area, Cape Smith Belt, New Quebec. Mineral Deposits of Canada: A Synthesis of Major Deposit-Types, District Metallogeny, The Evolution of Geological Provinces, and Exploration Methods 5, 351–386.
Lesher, C.M., Thibert, F., Gillies, S.L., Stilson, C.M., Thacker, J.L., Williams, D.A., 1999. Lithology and physical volcanology of komatiitic peridotite-gabbro complexes in the Raglan Block. In: Lesher, C.M. (Ed.), Komatiitic Peridotite-Hosted Fe-Ni-Cu-(PGE) Sulphide Deposits in the Raglan Area. Laurentian University, Cape Smith Belt, New Quebec.
Machado, N., Clark, T., David, J., Goulet, N., 1997. U-Pb ages for magmatism and deformation in the New Quebec Orogen. Can. J. Earth Sci. 34, 716–723.
Maurice, C., Francis, D., 2010. Enriched crustal and mantle components and the role of the lithosphere in generating Paleoproterozoic dyke swarms of the Ungava Peninsula, Canada. Lithos 114, 95–108.
Mayborn, K.R., Lesher, C.E., 2004. Paleoproterozoic mafic dike swarms of northeast Laurentia: products of plumes or ambient mantle? Earth Planet. Sci. Lett. 225 (3–4), 305–317.
McDonough, W.F., Sun, S.-S., 1995. The composition of the Earth. Chem. Geol. 120, 223–253.
McKenzie, D., Bickle, M.J., 1988. The volume and composition of melt generated by extension of the lithosphere. J. Petrol. 29, 625–679.
Minifie, M.J., Kerr, A.C., Ernst, R.E., Hastie, A.R., Ciborowski, T.J.C., Desharnais, G., Milliar, I.L., 2013. The northern and southern sections of the western ca. 1880 Ma Circum-Superior Large Igneous Province, North America: The Pickle Crow dyke connection? Lithos 174, 217–235.
Mungall, J.E., 2007. Crustal contamination of picritic magmas during transport through dikes: the Expo Intrusive Suite, Cape Smith Fold Belt, New Quebec. J. Petrol. 48, 1021–1039.
Nebel, O., Arculus, R.J., Ivanic, T.J., Nebel-Jacobsen, Y.J., 2013. Lu–Hf isotopic memory of plume–lithosphere interaction in the source of layered mafic intrusions, Windimurra Igneous Complex, Yilgarn Craton, Australia. Earth Planet. Sci. Lett. 380, 151–161.
Nebel, O., Campbell, I.A., Sossi, P.A., Van Kranendonk, M.J., 2014. Hafnium and iron isotopes in early Archean komatiites record a plume-driven convection cycle in the Hadean Earth. Earth Planet. Sci. Lett. 397, 111–120.
Nielsen, R.L., Gallahan, W.E., Newberger, F., 1992. Experimentally determined mineral-melt partition coefficients for Sc, Y and REE for olivine, orthopyroxene, pigeonite, magnetite and ilmenite. Contrib. Miner. Petrol. 110, 488–499.
Ohta, H., Maruyama, S., Takahashi, E., Watanabe, Y., Kato, Y., 1996. Field occurrence, geochemistry and petrogenesis of the Archean mid-oceanic ridge basalts (AMORBs) of the Cleaverville area, Pilbara craton, Western Australia. Lithos 37, 199–221.
Ojakangas, R.W., Morey, G.B., Southwick, D.L., 2001. Paleoproterozoic basin development and sedimentation in the Lake Superior region, North America. Sed. Geol. 141–142, 319–341.
Paktunc, A.D., 1984. Metamorphism of the ultramafic rocks of the Thompson mine, Thompson Nickel Belt, northern Manitoba. Can. Mineral. 22, 77–91.
Paktunc, A.D., 1987. Differentiation of the Cuthbert Lake ultramafic dikes and related mafic dikes. Contrib. Miner. Petrol. 97, 405–416.
Parrish, R.R., 1989. U-Pb geochronology of the Cape Smith Belt and Sugluk block, northern Quebec. Geosci. Can. 16, 126–130.
Pearce, J.A., 1996. A user's guide to basalt discrimination diagrams. In: Trace element geochemistry of volcanic rocks: application for massive sulphide exploration. In: Wyman, D. (Ed.), . Geological Association of Canada Short Course Notes, vol. 12. Geological Association of Canada, Mineral Deposits Division, Winnipeg, pp. 79–113.
Pearce, J.A., Peate, D.W., 1995. Tectonic implications of the composition of volcanic arc magmas. Annu. Rev. Earth Planet. Sci. 23, 251–285.
Percival, J.A., Whalen, J.B., Rayner, N., 2004. Pikwitonei-Snow Lake, Manitoba transect (parts of NTS 63J, 63O and 63P), Trans-Hudson Orogen-Superior Margin Metallotect Project: initial geological, isotopic and SHRIMP U-Pb results. In: Report of Activities 2004. Manitoba Industry, Economic Development and Mines, Manitoba Geological Survey, Winnipeg, pp. 120–134.
Percival, J.A., Whalen, J.B., Rayner, N., 2005. Pikwitonei-Snow Lake, Manitoba transect (parts of NTS 63J, 63O and 63P), Trans-Hudson Orogen-Superior Margin Metallotect Project: new results and tectonic interpretation. In: Report of Activities 2005. Manitoba Industry, Economic Development and Mines, Manitoba Geological Survey, Winnipeg, pp. 69–91.
Peredery, W.V., 1982. Geology and nickel sulphide deposits of the Thompson Belt, Manitoba. In: Precambrian sulphide deposits. In: Hutchison, R.W., Spence, C.D., Franklin, J.M. (Eds.), . Geological Association of Canada Special Paper 2, vol. 5. Geological Association of Canada, Toronto, pp. 165–209.
Picard, C., Lamothe, D., Piboule, M., Oliver, R., 1990. Magmatic and geotectonic evolution of a Proterozoic oceanic basin system: the Cape Smith Thrust-Fold Belt (New Quebec). Precambr. Res. 47, 223–249.
Pietrzak-Renaud, N., Davis, D., 2014. U-Pb geochronology of baddeleyite from the Belleview metadiabase: Age and geotectonic implications for the Negaunee Iron Formation, Michigan. Precambr. Res. 250, 1–5.
Randall, W., 2005. U-Pb geochronology of the Expo Igneous Suite, Cape Smith Belt, and the Kyak Bay intrusion, New Quebec Orogen: implications for the tectonic evolution of the northeastern Trans- Hudson Orogen MSc thesis. University of Toronto, Toronto. 51pp.
Richter, F.M. 1988. A major change in the thermal state of the Earth at the Archean-Proterozoic boundary: consequences for the nature and preservation of continental lithosphere. J. Petrol., Special Lithosphere Issue, 39–52.
Ricketts, B.D., Donaldson, J.A., 1981. Sedimentary history of the Belcher Group of Hudson Bay. In: Campbell, F.H.A. (Ed.), Proterozoic basins of Canada. Geological Survey of Canada Paper 81-10. Geological Survey of Canada, Ottawa, pp. 235–254.
Ricketts, B.D., Ware, M.J., Donaldson, J.A., 1982. Volcaniclastic rocks and volcaniclastic facies in the middle Precambrian (Aphebian) Belcher Group, Northwest Territories, Canada. Can. J. Earth Sci. 19, 1275–1294.
Rohon, M.L., Vialette, Y., Clark, T., Roger, G., Ohnenstetter, D., Vidal, P., 1993. Aphebian mafic- ultramafic magmatism in the Labrador Trough (New Quebec): its age and nature of its mantle source. Can. J. Earth Sci. 30, 1582–1593.
Rudnick, R.L., Fountain, D.M., 1995. Nature and composition of the continental crust: a lower crustal perspective. Rev. Geophys. 33, 267–309.
Rudnick, R. L., Gao, S., 2003. 3.01 – Composition of the Continental Crust. In Treatise on Geochemistry, eds. D. H. Editors-in-Chief: Heinrich and K. T. Karl, 1–64. Oxford: Pergamon.
Rukhlov, A.S., Bell, K., 2010. Geochronology of carbonatites from the Canadian and Baltic Shields, and the Canadian Cordillera: clues to mantle evolution. Mineral. Petrol. 98, 11–54.
Sage, R.P., 1988. Geology of carbonatite-alkalic rock complexes in Ontario: Cargill Township carbonatite complex, district of Cochrane. Ontario Geological Survey Study 36. Ministry of Northern Development and Mines, Mines and Minerals Division, Toronto. 92pp.
Sage, R.P., 1988. Geology of carbonatite-alkalic rock complexes in Ontario: Goldray carbonatite complex, district of Cochrane. Ontario Geological Survey Study 40. Ministry of Northern Development and Mines, Mines and Minerals Division, Toronto. 35pp.
Said, N., Kerrich, R., Groves, D., 2010. Geochemical systematics of basalts of the Lower Basalt Unit, 2.7 Ga Kambalda Sequence, Yilgarn craton, Australia: plume impingement at a rifted craton margin. Lithos 115, 82–100.
Salters, V.J.M., Zindler, A., 1995. Extreme 176Hf/177Hf in the sub-oceanic mantle. Earth Planet. Sci. Lett. 129, 13–30.
Saunders, A.D., England, R.W., Reichow, M.K., White, R.V., 2005. A mantle plume origin for the Siberian traps: uplift and extension in the West Siberian Basin, Russia. Lithos 79, 407–424.
Schmidt, P.W., Williams, G.E., 2003. Reversal asymmetry in Mesoproterozoic overprinting of the 1.88 Ga Gunflint Formation, Ontario, Canada: non-dipole effects or apparent polar wander? Tectonophysics 377, 7–32.
Scoates, R.F.J. 1981. Volcanic rocks of the Fox River Belt, northeastern Manitoba. Geological Report GR81-1. Manitoba Department of Energy and Mines, Mineral Resources Division, Winnipeg. 109pp.
Schneider, D.A., Bickford, M.E., Cannon, W.F., Schulz, K.J., Hamilton, M.A., 2002. Age of volcanic rocks and syndepositional iron formations, Marquette Range Supergroup: implications for the tectonic setting of Paleoproterozoic iron formations of the Lake Superior region. Can. J. Earth Sci. 39, 999–1012.
Schulz, K.J., Cannon, W.F., 2007. The Penokean orogeny in the Lake Superior region. Precambr. Res. 157, 4–25.
Schwarz, E.J., Freda, G.N., 1983. Paleomagnetism and time-stratigraphic correlation of Proterozoic redbeds of the Labrador Trough and outliers of northern Quebec. Can. J. Earth Sci. 20, 1725–1737.
Scoates, R.F.J., Macek, J.J. 1978. Molson dyke swarm. Geological Paper 78–1. Manitoba Department of Mines, Resources and Environmental Management, Mineral Resources Division, Geological Survey, Winnipeg. 53pp.
Scoates, R.F.J., Macek, J.J., Russell, J.K., 1977. Thompson Nickel Belt project (parts of 63P–13NE, 63P–14NW, 63P–12SW and 63O–9NE). In: Report of Activities 1977. Manitoba Department of Mines, Resources and Environmental Management, Mineral Resources Division, Geological Survey, Winnipeg, pp. 47–54.
Sims, P.K., 1990. Geologic map of Precambrian rocks of Iron Mountain and Escanaba $1^\circ \times 2^\circ$ quadrangles, northeastern Wisconsin and northwestern Michigan. US Geological Survey Miscellaneous Investigations Series Map I-2056.
Skulski, T., Wares, R.P., Smith, A.D., 1993. Early Proterozoic (1.88-1.87 Ga) tholeiitic magmatism in the New Quebec Orogen. Can. J. Earth Sci. 30, 1505–1520.
Sleep, N.H., Ebinger, C.J., Kendall, J.-M., 2002. Deflection of mantle plume material by cratonic keels. In: The early Earth: physical, chemical and biological development. In: Fowler, C.M.R., Ebinger, C.J., Hawkesworth, C.J. (Eds.), . Geological Society Special Publication, vol. 199. Geological Society of London, London, pp. 135–150.
Sobolev, S.V., Sobolev, A.V., Kuzmin, D.V., Krivolutskaya, N.A., Petrunin, A.G., Arndt, N.T., Radko, V.A., Vasiliev, Y.R., 2011. Linking mantle plumes, large igneous provinces and environmental catastrophes. Nature 477, 312–316.
Soderlund, U., Hofmann, A., Klausen, M.B., Olsson, J.R., Ernst, R.E., Persson, P.-O., 2010. Towards a complete magmatic barcode for the Zimbabwe craton: baddeleyite U-Pb dating of regional dolerite dyke swarms and sill complexes. Precambr. Res. 183, 388–398.
Sol, S., Thomson, C.J., Kendall, J.-M., White, D., VanDecar, J.C., Asudeh, I., 2002. Seismic tomographic images of the cratonic upper mantle beneath the western Superior Province of the Canadian Shield – a remnant Archean slab? Phys. Earth Planet. Inter. 134, 53–69.
Staudigel, H. et al., 1996. Geochemical fluxes during seafloor alteration of the basaltic upper oceanic crust: Dsdp Sites 417 and 418. Subduction Top to Bottom. American Geophysical Union, pp. 19–38.

St-Onge, M.R., Lucas, S.B., Parrish, R.R., 1992. Terrane accretion in the internal zone of the Ungava orogen, northern Quebec. Part 1: tectonostratigraphic assemblages and their tectonic interpretations. Can. J. Earth Sci. 29, 746–764.
St-Onge, M.R., Scott, D.J., Lucas, S.B., 2000. Early partitioning of Quebec: microcontinent formation in the Paleoproterozoic. Geology 28, 323–326.
Stracke, A. et al., 2003. Recycling oceanic crust: Quantitative constraints. Geochem. Geophys. Geosys. 4 (3).
Sun, S.-S., McDonough, W.F., 1989. Chemical and isotopic systematics of oceanic basalts: implications for mantle composition and processes. In: Magmatism in the ocean basins. In: Saunders, A.D., Norry, M.J. (Eds.), . Geological Society Special Publication, vol. 42. Geological Society of London, London, pp. 313–345.
Thompson, R.N., Gibson, S.A., 1991. Subcontinental mantle plumes, hotspots and pre-existing thinspots. J. Geol. Soc. London 148, 973–977.
Todt, W., Chauvel, C., Arndt, N.T., Hofmann, A.W., 1984. Pb isotopic composition and age of Proterozoic komatiites and related rocks from Canada. American Geophysical Union Fall Meeting 1984. Program with Abstracts 65, pp. 1129.
Ueng, W.C., Fox, T.P., Larue, D.K., Wilband, J.T., 1988. Geochemistry and petrogenesis of the early Proterozoic Hemlock volcanic rocks and the Kiernan sills, southern Lake Superior region. Can. J. Earth Sci. 25, 528–546.
van der Lee, S., Nolet, G., 1997. Upper mantle S velocity structure of North America. J. Geophys. Res. 102, 22815–22838.
Vervoort, J.D., Blichert-Toft, J., 1999. Evolution of the depleted mantle: Hf isotope evidence from juvenile rocks through time. Geochim. Cosmochim. Acta 63, 533–556.
Walter, M.J., 1998. Melting of garnet peridotite and the origin of komatiite and depleted lithosphere. J. Petrol. 39, 29–60.
Waterton, P., Person, D.G., Kjarsgaard, B., Hulbert, L., Locock, A., Parman, S., David, D., 2017. Age, origin, and thermal evolution of the ultra-fresh ~1.9 Ga Winnipegosis Komatiites, Manitoba, Canada. Lithos 268–271, 114–130.
Wier, K.L., 1967. Geology of the Kelso Junction quadrangle, Iron County, Michigan. US Geological Survey Bulletin 1226. US Government Printing Office, Washington DC. 47pp.
Wodicka, N., Madore, L., Larbi, Y., Vicker, P., 2002. Géochronologie U-Pb de filons-couches mafiques de la Ceinture de Cape Smith et de la Fosse du Labrador. In: L'exploration minérale au Québec: notre savoir, vos découvertes. Séminaire d'information sur la recherche géologique. Programme et résumés 2002–10. Ministère des Ressources Naturelles, Québec. 48pp.
Wolfe, C.J., Bjarnason, I.T., VanDecar, J.C., Solomon, S.C., 1997. Seismic structure of the Iceland mantle plume. Nature 385, 245–247.
Workman, R.K., Hart, S.R., 2005. Major and trace element composition of the depleted MORB mantle (DMM). Earth Planet. Sci. Lett. 231, 53–72.
Zwanzig, H.V., Bohm, C.O., Protrel, A., Machado, N., 2003. Field relations, U-Pb zircon ages and Nd model ages of granitoid intrusions along the Thompson Nickel Belt-Kisseynew Domain boundary, Setting Lake area, Manitoba (NTS 63J15 and 63O2). In: Report of Activities 2003. Manitoba Industry, Economic Development and Mines, Manitoba Geological Survey, Winnipeg, pp. 118–129.